Draft version June 23, 2026
Typeset using LaTeX default style in AASTeX631

Hubble constant constraint using 117 FRBs with a more accurate probability density function for $\mathrm{DM_{diff}}$

Jiaming Zhuge(诸葛佳明) [1,2,*] Marios Kalomenopoulos [1,2,†] and Bing Zhang(张冰) [1,2,‡]

[1] Nevada Center for Astrophysics, University of Nevada, Las Vegas, NV 89154, USA
[2] Department of Physics and Astronomy, University of Nevada, Las Vegas, NV 89154, USA

ABSTRACT

Fast radio bursts (FRBs) are among the most mysterious astronomical transients. Due to their short durations and cosmological distances, their dispersion measure (DM) - redshift (z) relation is useful for constraining cosmological parameters and detecting the baryons in the Universe. The increasing number of localized FRBs in recent years has provided more precise constraints on these parameters. However, the larger dataset reveals limitations in the widely used probability density function ($p_{\rm diff}$) for $\mathrm{DM_{diff}}$, which refers to the diffuse electron term of FRB DM. In this project, we collect 117 of the latest, localized FRBs, discuss the effect of a more accurate $\sigma_{\rm diff}$, which is a parameter in $p_{\rm diff}$ and once thoughts as "effective standard deviation", and more clearly rewrite their likelihood to better constrain the parameters above. We find that the widely used approximation $\sigma_{\rm diff} \sim F/\sqrt{z}$ only works under contrived assumptions and shows the greatest deviation from the true standard deviation in low redshift. In general, one should use an accurate method to derive this parameter from $p_{\rm diff}$. Our method yields better constraints on $H_0 \Omega_b f_{\rm diff} = 2.813^{+0.250}_{-0.258}$ km/s/Mpc or $H_0 = 66.889^{+6.754}_{-5.459}$ km/s/Mpc when combining the FRB data with CMB measurements and taking $f_{\rm diff} = 0.84$. This fully analytical correction helps us better constrain cosmological parameters with the increasing number of localized FRBs available today.

Keywords: Radio bursts (1339) — Radio transient sources (2008) — Hubble constant (758) — Baryon density (139) — Galaxy dark matter halos (1880) — Intergalactic medium (813)

1. INTRODUCTION

Fast radio bursts (FRBs) are millionsecond duration bursts first discovered by Lorimer et al. (2007). Predominantly located at cosmological distances, these radio bursts have very high brightness temperatures and luminosities (Thornton et al. 2013). Their dispersion measure (DM)-redshift dependence (Section 2) provides an independent way to study cosmological parameters, as well as the cosmic baryon distribution. (for reviews on FRBs, see e.g. Katz 2018; Popov et al. 2018; Cordes & Chatterjee 2019; Petroff et al. 2019; Platts et al. 2019; Zhang 2020; Xiao et al. 2021; Xiao et al. 2022; Petroff et al. 2022; Zhang 2023, 2024)

The early idea of using FRB DM to constrain cosmological parameters can be traced back to Deng & Zhang (2014); Gao et al. (2014); Zhou et al. (2014) (see also earlier discussion of DM-z relation of cosmological sources in general (Ioka 2003; Inoue 2004)), who only considered possible association events (for example, FRBs possibly associated with GRB events) or mock events due to the lack of localized FRBs. The breakthrough happened in 2020, when Macquart et al. (2020) used 5 localized FRBs, their "golden sample", together with physically motivated DM PDFs, to constrain cosmological parameters and astrophysical properties of the FRB sources.

With the increasing number of localized FRBs, FRB cosmology has become a popular topic in transient astronomy (e.g. Baptista et al. 2024; Kalita et al. 2024; Connor et al. 2025; Sharma et al. 2025; Wang et al. 2025; Xu et al. 2025; Acharya & Beniamini 2025). However, cosmological constraints from the new, localized FRBs always show much larger values of the parameter F. This parameter was once thought to quantify the effective standard deviation through

* jiaming.zhuge@unlv.edu
† marios.kalomenopoulos@gmail.com
‡ bing.zhang@unlv.edu

the relation $\sigma_{\rm diff} \sim F/\sqrt{z}$, where $\sigma_{\rm diff}$ is a parameter in the probability density function ($p_{\rm diff}$) of the diffuse electron dispersion measure ($\rm DM_{diff}$)(see the detailed discussion in Section 4.2). This problem is urgent and has attracted attention in the community. Results from Zhang et al. (2021) implied that the power of z in $\sigma_{\rm diff} \sim F/\sqrt{z}$ may be smaller according to the TNG300 dataset, simulated from IllustrisTNG (Nelson et al. 2019). Baptista et al. (2024) found that the IllustrisTNG simulations tend to underpredict F for small redshifts ($z < 0.4$), and importantly showed that the parameter is degenerate with H_0. Connor et al. (2025) argued that the F parameterization fails to adequately consider the contribution of IGM structure, such as the intersection of filaments and voids, while Sharma et al. (2025) quantified the inaccuracies of the Macquart PDF by analyzing hydrodynamical simulations with different feedback strengths. They found that the F parameter misestimates the variance of the PDF in the redshift range $0 < z < 2$, and eventually they proposed a new log-normal PDF for modeling the $\rm DM_{diff}$.

Cosmological simulations also call for modifications in the PDF, but the results are under debate. Takahashi et al. (2021) first compared different mass resolution runs of the TNG300 dataset, comparing simulated DM statistics with analytical ones. They found that the standard deviation of the DM calculated from the simulations $\sigma_{\rm DM}$ over the square-root of redshift remains constant with time, i.e., $\sigma_{\rm DM}/\sqrt{z} \sim 230 {\rm pc/cm^3}$. Medlock et al. (2025) studied, among other things, the evolution of the F parameter with time across different simulations—IllustrisTNG (Nelson et al. 2019), SIMBA (Davé et al. 2019), and Astrid (Ni et al. 2022) from the CAMELS (Villaescusa-Navarro et al. 2021) suite—observing it remains largely constant across the redshift range $z = 0-2$. This is in contrast with Zhang et al. (2021), who found that F is diverging for low-z in the IllustrisTNG simulation. Ziegler et al. (2024) provided a new fitting result from CoDa II (Ocvirk et al. 2020), where they investigated the evolution of DM and its standard deviation $\sigma_{\rm DM}$ to higher redshifts ($z \leq 12$).

In this paper, we derive the parameter $\sigma_{\rm diff}$ in $p_{\rm diff}$ from the true standard deviation to get more precise result in Section 4.2, based only on more accurate equations analytically. We also show the FRB DM likelihood in Section 4.3. These two consideration help us to get better constraints. We first review the idea of FRB cosmology in Section 2. In Section 3, we introduce our 117 latest localized FRBs' dataset and how we preprocess them. The key points of this paper are presented in Section 4, where we show the PDFs used in this work and how we consider the critical parameters $\sigma_{\rm diff}$. We also derive a clear form of the modified convolution to calculate the likelihood. In Section 5, we show all of our novel constraints, and the conclusions are summarized in Section 6.

2. FROM DM TO COSMOLOGY

The DM is connected to the difference of the arrival times of the electromagnetic waves in different frequencies when the waves propagate through an ionized gas. For two photons traveling from a cosmological distance of redshift z, with frequencies ν_1 and ν_2 much greater than the plasma frequency ω_p, their arrival time difference in the observer frame is (Rybicki & Lightman 1979; Deng & Zhang 2014):

$$\Delta t = \frac{e^2}{2\pi mc}\left(\frac{1}{\nu_1^2} - \frac{1}{\nu_2^2}\right)\int_0^L \frac{n_e(z)}{1+z}\,{\rm d}l\,. \tag{1}$$

Here, n_e is the number density of electrons, L is the proper distance from the FRB source to the observer. The dispersion measure is defined as the final integration term:

$$\mathrm{DM} = \int_0^L \frac{n_e(z)}{1+z}\,{\rm d}l\,. \tag{2}$$

The DM of an FRB is composed of the following three components ordered from local to distant (e.g. Thornton et al. 2013; Deng & Zhang 2014; Gao et al. 2014; Prochaska & Zheng 2019; James et al. 2021):

$$\mathrm{DM_{FRB}} = \mathrm{DM_{MW}} + \mathrm{DM_{diff}} + \frac{\mathrm{DM_{host}}}{1+z}. \tag{3}$$

Here, $\rm DM_{MW}$ is the Milky Way component, which consists of $\rm DM_{MW,ISM}$ and $\rm DM_{MW,halo}$, which are the interstellar medium and the Milky Way halo terms, respectively. The term $\rm DM_{MW,ISM}$ can be calculated with the Galactic electron models such as NE2001 (Cordes & Lazio 2002; Cordes & Lazio 2003) and YMW16 (Yao et al. 2017), which are derived from pulsar data. $\rm DM_{diff}$ is the contribution of diffuse electrons, which is the sum of DM in the intergalactic medium (IGM) ($\rm DM_{IGM}$) and DM in cosmic halos ($\rm DM_{halo}$). $\rm DM_{host}$ is the host environment term, which includes the contribution from the FRB's host galaxy and the immediate source environment ($\mathrm{DM_{src}}$). Note that $\mathrm{DM_{host}}$ is corrected by a factor of $(1+z)$ due to its cosmological distance.

$\mathrm{DM_{diff}}$ is the core component when inferring cosmology and the baryon distribution in the Universe. In ΛCDM cosmology, the mean value of the dispersion measure of diffuse matter can be written as (Deng & Zhang 2014; Gao et al. 2014; Zhou et al. 2014; Macquart et al. 2020):

$$\langle \mathrm{DM_{diff}} \rangle (z) = \frac{3cH_0\Omega_b}{8\pi G m_p} \int_0^z \frac{f_{\mathrm{diff}}(z')\chi(z')(1+z')}{\sqrt{\Omega_m(1+z')^3+\Omega_\Lambda}} \mathrm{d}z' \,, \tag{4}$$

with

$$\chi(z) = Y_H X_{e,H}(z) + \frac{1}{2} Y_p X_{e,He}(z) \tag{5}$$

We take $\langle \mathrm{DM_{diff}} \rangle$ to identify the theoretical $\mathrm{DM_{diff}}$. Here, Ω_b is the dimensionless baryon mass fraction of the Universe, f_{diff} is the fraction of the diffuse baryons in both IGM and halos, $\chi(z)$ is the fraction of ionized electrons to baryons and can be expanded as in Eq. 5, Y is the mass fraction of hydrogen or helium, and X is the ionization fraction for each element. In the low-redshift universe ($z<3$), both H and He are fully ionized, i.e. $\chi(z) \sim 7/8$ (Deng & Zhang 2014).

$\mathrm{DM_{diff}}$ is a function of redshift. It is related to the baryon distribution f_{diff}, the ionized fraction χ and the cosmological parameters H_0, Ω_b. This means that additionally to the comic microwave background or type-Ia supernovae, the $\mathrm{DM_{diff}}$ is another cosmic probe to study the different fractions of the components in the universe, as well as its reionization history.

3. DATA

In this project we collect the 117 latest localized FRBs with their redshifts and DM (Table 3) (e.g. Xu et al. 2023; Connor et al. 2025; Shannon et al. 2025; Scott et al. 2025). We deduct the term $\mathrm{DM_{MW,ISM}}$ using the NE2001 model (Cordes & Lazio 2002; Cordes & Lazio 2003), each calculated individually for each FRB based on its sky localization. $\mathrm{DM_{MW,halo}}$, according to previous studies, ranges from $30\,\mathrm{pc/cm^3}$ to $80\,\mathrm{pc/cm^3}$ (Xu & Han 2015; Dolag et al. 2015; Prochaska & Zheng 2019; Yamasaki & Totani 2020; Arcus et al. 2020; Hashimoto et al. 2020). In this project we take $\mathrm{DM_{MW,halo}} \sim 30\,\mathrm{pc/cm^3}$ for two reasons. First, a small $\mathrm{DM_{MW,halo}}$ will result in more positive $\mathrm{DM_{ext}}$ and retain more data with physical DM values to constrain. Second, the add-on value of $\mathrm{DM_{MW,halo}}$ can be absorbed in the other DM components, if our assumed value proves too small. The standard deviations in $\mathrm{DM_{MW,halo}}$ and $\mathrm{DM_{MW,ISM}}$ will be absorbed in the standard deviation of $\mathrm{DM_{host}}$. Thus, we can define the extragalactic $\mathrm{DM_{ext}}$ as the observed DM ($\mathrm{DM_{obs}}$) subtracting the MW term, such that $\mathrm{DM_{ext}}$ includes the diffuse electron term and host environment term:

$$\mathrm{DM_{ext}} = \mathrm{DM_{obs}} - \mathrm{DM_{MW,halo}} - \mathrm{DM_{MW,ISM}} = \mathrm{DM_{diff}} + \frac{\mathrm{DM_{host}}}{1+z} \tag{6}$$

For all FRBs, a linear least squares fit yields:

$$\mathrm{DM_{ext}} = \mathrm{DM} - \mathrm{DM_{MW}} = (975.27z + 123.06)\ \mathrm{pc/cm^3}. \tag{7}$$

The slope gives us a rough estimate for the parameters in $\langle \mathrm{DM_{diff}} \rangle (z)$, and the intercept reflects the value of $\mathrm{DM_{host}}$ (e.g. Zhang 2023). Our FRBs data sample and the linear fit function are shown in Fig. 1.

To prevent $\mathrm{DM_{src}}$ from being the dominant term, we drop two special FRBs, FRB 20190520B and FRB 20220831A, which have peculiarly high $\mathrm{DM_{ext}}$ but relatively small redshift. We also apply the redshift constraint $z \geq 0.25$, retaining 44 FRBs. This redshift cut is determined from our analysis of the PDF p_{diff} limits (see details in Section 4.2.1).

4. METHODS

After correcting for MW effects, the only two terms left are $\mathrm{DM_{diff}}$ and $\mathrm{DM_{host}}$. Here, we use the maximum likelihood method and Markov Chain Monte Carlo (MCMC) to study the parameters in the PDFs described below and constrain cosmology.

4.1. *PDF for Host galaxy term*

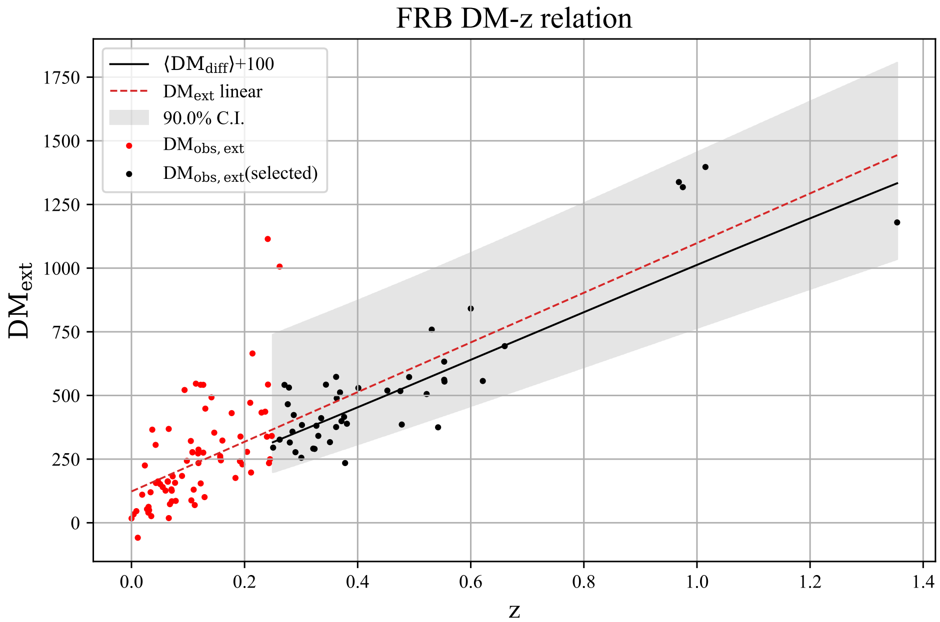

Figure 1. $\mathrm{DM_{ext}} - z$ relation for 117 localized FRBs, where $\mathrm{DM_{ext}} = \mathrm{DM} - \mathrm{DM_{MW}}$ is the extragalactic DM. The dashed red line is the best fitting linear function for all data, while the back line shows the theoretical line from Eq. 4 adding $100\,\mathrm{pc\,cm^{-3}}$ for $\mathrm{DM_{host}}$. We also show 90% confidence interval in shaded region calculated from our parameters searching results. The black data points are those FRBs $z \geq 0.25$ that $p_{\mathrm{diff}}(\Delta)$ worked within this range.

For $\mathrm{DM_{host}}$, we take a log-normal distribution:

$$p_{\mathrm{host}}(\mathrm{DM_{host}}|\mu, \sigma_{\mathrm{host}}) = \frac{1}{\sqrt{2\pi}\sigma_{\mathrm{host}}\mathrm{DM_{host}}} \exp\left[-\frac{(\ln \mathrm{DM_{host}} - \mu)^2}{2\sigma_{\mathrm{host}}^2}\right], \tag{8}$$

which has an asymmetric tail in the large value side. The asymmetric tail allows for the existence of a large value $\mathrm{DM_{host}}$, which may come from a dense local environment. The median value for this function is $\exp(\mu)$. The variance of this function is $[\exp(\sigma_{\mathrm{host}}^2) - 1]\exp(2\mu + \sigma_{\mathrm{host}}^2)$. We take $\exp(\mu)$ and σ_{host} as two unknown parameters to search for. Note that the variable $\mathrm{DM_{host}}$ here should be the value in the comoving frame because in Eq. 3 we divide $\mathrm{DM_{host}}$ by $(1 + z)$.

4.2. *PDF for Diffuse electron term*

For $\mathrm{DM_{diff}}$, we take the distribution:

$$p_{\Delta}(\Delta) = \mathcal{A}\Delta^{-\beta} \exp\left[-\frac{(\Delta^{-\alpha} - C_0)^2}{2\alpha^2\sigma_{\mathrm{diff}}^2}\right], \tag{9}$$

which was first used in (McQuinn 2013; Prochaska & Zheng 2019; Macquart et al. 2020) and was derived from modeling both observational and simulation data. Here, Δ refers to the dimensionless fraction between the measured and theoretical diffuse DM terms, which is $\Delta = \mathrm{DM_{diff}}/\langle\mathrm{DM_{diff}}\rangle$; $\mathcal{A}$ is the normalization factor, calculated imposing $\int p_{\Delta} d\Delta = 1$; C_0 is a factor that affects the mean value (Since this PDF is highly right-skewed, to find C_0 we impose the condition that the mean value of Δ equals to 1, which holds by definition $\langle\Delta\rangle = \langle\mathrm{DM_{diff}}\rangle/\langle\mathrm{DM_{diff}}\rangle = 1$); α and β are the parameters that describe the gas profile in cosmic halos and we adopt $\alpha = \beta = 3$ following Macquart et al. (2020); Finally σ_{diff} is related to the scatter of Δ and is redshift-dependent.

4.2.1. *A more accurate σ_{diff} and the limitation of F*

$\sigma_{\mathrm{diff}} \sim F/\sqrt{z}$ was once thought to be the "effective standard deviation"(Macquart et al. 2020). However, in this PDF form, σ_{diff} may deviate greatly from the true standard deviation of Δ. To prevent any confusion, we define a new variable σ_{Δ} as the true standard deviation to differentiate it from σ_{diff}. An easy way to estimate σ_{Δ} is to consider its contributions from the intergalactic medium and halos, since $\mathrm{DM_{diff}} = \mathrm{DM_{IGM}} + \mathrm{DM_{halos}}$. Because Δ is $\mathrm{DM_{diff}}$ normalized by its theoretical result $\langle \mathrm{DM_{diff}} \rangle$, the standard deviation of Δ can be written as $\sigma_\Delta \sim \sqrt{(\sigma^2_{\mathrm{IGM}} + \sum_i \sigma^2_{\mathrm{halo,i}})/\langle \mathrm{DM_{diff}} \rangle^2}$. Here, $\sigma_{\mathrm{halos,i}}$ stands for the standard deviation contribution of each halo along the line of sight from the FRB source to the Milky Way. For sufficiently large distances, the sum of $\sigma_{\mathrm{halos,i}}$ will dominate the standard deviation (the IGM-dominated case is shown in Eq. 19). To simplify the quantity, we define their mean square as

$$\overline{\sigma^2}_{\mathrm{halo}} \sim 1/N \cdot \sum_i \sigma^2_{\mathrm{halo,i}}, \tag{10}$$

where N is the total number of halos along the line of sight. At a substantial distance, $\mathrm{DM_{halos}}$ is approximately equal to the product of the number density of halos n_{halo} (in the comoving volume), the comoving distance to the source of the FRB D_c, and the typical cross section of the halo A_{halo}. One can define a "mean observed halo path" as $l \sim 1/(n_{\mathrm{halo}} A_{\mathrm{halo}})$. Thus the number of halos in the line of sight, $N \sim n_{\mathrm{halo}} A_{\mathrm{halo}} D_c \sim D_c/l$, is approximately the distance to the FRB source over the typical distance for one halo, and has a substantial DM standard deviation contribution with

$$\sigma_\Delta \sim \sqrt{\frac{\sigma^2_{\mathrm{IGM}} + \sum_i \sigma^2_{\mathrm{halo,i}}}{\langle \mathrm{DM_{diff}} \rangle^2}} \sim \sqrt{\frac{N \overline{\sigma^2}_{\mathrm{halo}}}{\langle \mathrm{DM_{diff}} \rangle^2}} \sim \sqrt{\frac{\overline{\sigma^2}_{\mathrm{halo}} n_{\mathrm{halo}} A_{\mathrm{halo}} D_c}{\langle \mathrm{DM_{diff}} \rangle^2}} \sim \sqrt{\frac{\overline{\sigma^2}_{\mathrm{halo}} D_c}{\langle \mathrm{DM_{diff}} \rangle^2 l}}. \tag{11}$$

We can further expand this result by recalling Eq. 4 and the definition of comoving distance $D_c = c/H_0 \int_0^z \mathrm{d}z'/E(z')$ (Hogg 2000). For convenience, we define $E(z) = \sqrt{\Omega_m (1+z)^3 + \Omega_\Lambda}$ (in ΛCDM cosmology). As for l, we can take $n_{\mathrm{halo}} \sim 10^{-3}\,\mathrm{Mpc}^{-3}$ and $A_{\mathrm{halo}} \sim 1\,\mathrm{Mpc}^2$ to get an order of magnitude estimation $l \sim 1/(n_{\mathrm{halo}} A_{\mathrm{halo}}) \sim 1\mathrm{Gpc}$ (Press & Schechter 1974; Longair 2023; Zhang et al. 2025b). If we write σ_Δ as a function of the redshift z, we can absorb all constants into a parameter S to get

$$\sigma_\Delta \sim \frac{64\pi G m_p}{21\sqrt{c}} \sqrt{\frac{\overline{\sigma^2}_{\mathrm{halo}}}{H_0^3 \Omega_b^2 f_{\mathrm{diff}}^2 l}} \frac{\sqrt{\int_0^z \mathrm{d}z'/E(z')}}{\int_0^z (1+z')\,\mathrm{d}z'/E(z')} \tag{12}$$

$$\sim \sqrt{0.115} \left(\frac{H_0}{67\,\mathrm{km\,s^{-1}\,Mpc^{-1}}}\right)^{-\frac{3}{2}} \left(\frac{\Omega_b}{0.04897}\right)^{-1} \left(\frac{f_{\mathrm{diff}}}{0.84}\right)^{-1} \left(\frac{\overline{\sigma^2}_{\mathrm{halo}}}{(130\ \mathrm{pc\,cm^{-3}})^2}\right)^{\frac{1}{2}} \left(\frac{l}{1\mathrm{Gpc}}\right)^{-\frac{1}{2}} \frac{\sqrt{\int_0^z \mathrm{d}z'/E(z')}}{\int_0^z (1+z')\,\mathrm{d}z/E(z')} \tag{13}$$

$$\sim \frac{\sqrt{S \int_0^z \mathrm{d}z'/E(z')}}{\int_0^z (1+z')\,\mathrm{d}z/E(z')}. \tag{14}$$

Note that the values n_{halo} and A_{halo} used here are only rough estimates, as they are actually functions of mass and redshift. The realistic values for l should be obtained by integrating the relation $l \sim 1/(n_{\mathrm{halo}} A_{\mathrm{halo}})$ over the redshift distribution of halos along the line of sight.

The equation also shows $S \propto \overline{\sigma^2}_{\mathrm{halo}}/(H_0^3 \Omega_b^2 f_{\mathrm{diff}}^2 l)$. If we understand more details about the astrophysical properties and distribution of halos, especially the parameters $\overline{\sigma^2}_{\mathrm{halo}}$ and l, $\sigma_\Delta(S, z)$ can in principle provide a new way to constrain cosmological parameters.

When the redshift is much smaller than 1 ($z \ll 1$), this formula finally returns to the same form as in Macquart et al. (2020):

$$\sigma_\Delta \sim \frac{\sqrt{S \int_0^z \mathrm{d}z'/E(z')}}{\int_0^z (1+z')\,\mathrm{d}z/E(z')} \tag{15}$$

$$\overset{z \ll 1}{\sim} \frac{\widetilde{F}}{\sqrt{z}}. \tag{16}$$

However, the standard deviation σ_Δ is not always equal to the parameter σ_{diff} (Connor et al. 2025; Sharma et al. 2025). Thus we use symbol $\widetilde{F}$ rather than F (Macquart et al. 2020) to distinguish the standard deviation σ_Δ from σ_{diff} in p_{diff}. Also, because our data reach a maximum redshift of 1.354 for FRB 20230521B, in this work we use the full expression (Eq. 14) numerically integrating for a given redshift and the parameter S.

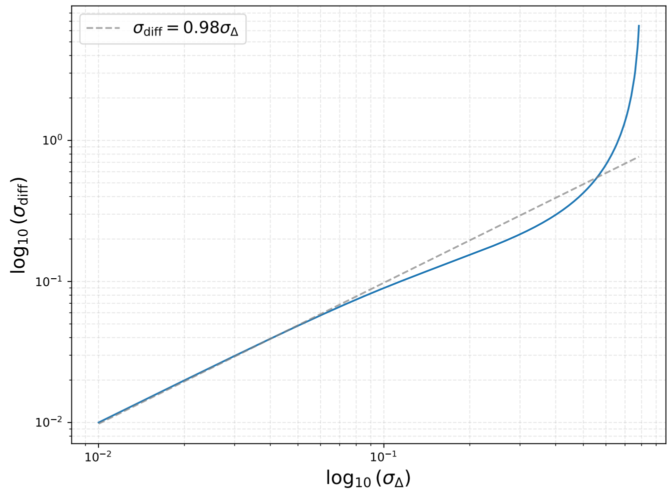

Figure 2. $\sigma_\Delta - \sigma_{\rm diff}$ relation in $\log_{10}$ space. The dashed black line is the best linear fitting line for the nearly linear part for $\sigma_{\rm diff}(\sigma_\Delta)$.

In order to find the relation between the standard deviation σ_Δ and the parameter $\sigma_{\rm diff}$, we derive σ_Δ from the 95% confidence interval to obtain $\sigma_{\rm diff}$. $\int_{\Delta_1}^{\Delta_2} p_\Delta(\Delta; \sigma_{\rm diff}) {\rm d}\Delta = 95.45\%$ where $\Delta_2 - \Delta_1 = 4\sigma_\Delta$. We numerically calculate the $\sigma_\Delta - \sigma_{\rm diff}$ relation and plot it in Fig. 2 in $\log_{10}$ space. In Fig. 2, if $\sigma_\Delta - \sigma_{\rm diff}$ is parallel with $\log_{10} y = \log_{10} x$, because $\sigma_\Delta \sim \widetilde{F}/\sqrt{z}$, $\sigma_{\rm diff}$ can be written as $F/\sqrt{z}$, where F includes some constant times $\widetilde{F}$. However, σ_Δ and $\sigma_{\rm diff}$ only show a linear relationship when $\sigma_\Delta \lesssim 0.60$ or $\sigma_{\rm diff} \lesssim 0.60$. From this region, we obtain the best-fitting function $\log_{10}\sigma_{\rm diff} = \log_{10}\sigma_\Delta - 0.00928$ or $\sigma_{\rm diff} = 0.979\sigma_\Delta$. Recall that when $z \ll 1$ in Macquart et al. (2020), $\sigma_{\rm diff} \sim F/\sqrt{z}$. Thus, we have the relation between the two parameters:

$$F \sim 0.979\widetilde{F} \sim 0.979\sqrt{S} \tag{17}$$

In other words, $\sigma_{\rm diff} = F/\sqrt{z}$ is correct only when the redshifts of the FRBs are not too small, within the range

$$\sigma_{\rm diff} = \frac{F}{\sqrt{z}} \lesssim 0.60 \;\Rightarrow\; z \gtrsim \left(\frac{F}{0.60}\right)^2. \tag{18}$$

On the other hand, only when $z \ll 1$, we have $\sigma_\Delta \sim \widetilde{F}$ or $\sigma_{\rm diff} \sim F/\sqrt{z}$. The two contradictory requirements imply $\widetilde{F}$ or F is not a good approximation. This is also the reason why we use S here. Eq. 17 actually only works for a very tight range (depending on the value S or F fit from the data). So Eq. 17 is only used to show the equivalent F value derived from S, to compare with the F value in previous research works.

For a given search range for F, $F/\sqrt{z}$ is only correct when z is not too small; otherwise, very small z will push $\sigma_{\rm diff}$ to grow rapidly and one must numerically consider the $\sigma_\Delta - \sigma_{\rm diff}$ relation. If not, the small redshift will favor a larger F in order to catch up with the real evolution of $\sigma_{\rm diff}$. This might explain why taking the latest FRB observation data would lead to finding a larger value of F on the boundary with a smaller cosmological parameter preference (Lin & Zou 2023).

When $D_c \ll l$ or redshift is very small, the $\sigma_{\rm IGM}$ term dominates (Eq. 11). This physically corresponds to the case, where the distance to the FRB is very close, so there are no intervening halos in between. Hence, we have:

$$\sigma_\Delta \sim \frac{\sigma_{\rm IGM}}{\langle {\rm DM_{diff}} \rangle} \tag{19}$$

$$\sim \sigma_{\rm IGM} \frac{64\pi G m_p}{21 c H_0 \Omega_b f_d} \frac{1}{\int_0^z (1+z')\,{\rm d}z' / E(z')} \tag{20}$$

$$\overset{z\ll 1}{\approx} \sigma_{\rm IGM} \frac{\widetilde{F}'}{z} = 0.002 \left(\frac{\sigma_{\rm IGM}}{100\ {\rm pc\,cm^{-3}}}\right) \frac{1}{z}. \tag{21}$$

Nevertheless, the even faster growth of $\sigma_\Delta(S, z)$ at small redshifts cannot resolve its limit in Fig. 2. This logarithmic divergence originates from the definition of the PDF $p_{\rm diff}(\Delta)$. When $z \to 0$, $\langle {\rm DM_{diff}} \rangle \to 0$ and causes the value of Δ

to fluctuate wildly. This is the reason why σ_Δ increases when $z \to 0$. With a larger standard deviation, the PDF will span a larger domain and $\sigma_{\rm diff}$ will increase accordingly. However, $p_{\rm diff}$ is a quasi-Gaussian distribution multiplied by $\Delta^{-\beta}$. When the parameter $\sigma_{\rm diff}$ in the second quasi-Gaussian distribution term increases, the probability at larger Δ will be suppressed by $\Delta^{-\beta}$. Thus in Fig. 2 we see that when $z \to 0$, the parameter $\sigma_{\rm diff}$ needs to grow even faster to make the standard deviation σ_Δ increase. Finally, no matter how fast $\sigma_{\rm diff}$ is growing, σ_Δ does not increase anymore and reaches a limit. On the other hand, when z is large enough, the $\Delta^{-\beta}$ term merely reshapes the PDF and the PDF will be more like a Gaussian distribution. σ_Δ and $\sigma_{\rm diff}$ will be more linear in this case and $\sigma_{\rm diff}$ can be recognized as the "effective standard deviation". Overall, the definition of $p_{\rm diff}(\Delta)$ naturally cannot handle the $z \to 0$ case and must have a minimum z limit. The parameters α and β will adjust the shape of $p_{\rm diff}(\Delta)$ and affect its applicable redshift range. Given that α and β are the parameters describing the gas density profile in the halos, the halo mass function and AGN feedback strength (Zhang et al. 2025b) will influence the parameters and finally change the applicable redshift range. This fact calls for detailed revisiting of $p_{\rm diff}(\Delta)$, especially α and β.

A comprehensive consideration of the gas density profile and revisiting the PDF are beyond this project. Hence, to expand the redshift domain where this function applies, in the following analysis we still consider the halo-dominated case in Eq. 14. We neglect the IGM-dominated case in the following sections and hope a more precise PDF at low redshift can use the standard deviation for the IGM term. We also perform a sample cut as mentioned in Section 3.

4.2.2. *Cosmological dependence of S or F*

The derivation of the standard deviation of Δ reveals the cosmological dependence of the S or F term, usually used in the Macquart relation. For $z \ll 1$, Eq. 16 becomes

$$\sigma_\Delta^2 \sim \frac{1}{H_0^3}\frac{1}{z}\frac{\overline{\sigma^2}_{\rm halo}}{l}\frac{(64\pi G m_p)^2}{c(21\Omega_b f_{\rm diff})^2}, \tag{22}$$

with S defined as

$$S \sim \widetilde{F}^2 \sim \frac{1}{H_0^3}\frac{\overline{\sigma^2}_{\rm halo}}{l}\frac{(64\pi G m_p)^2}{c(21\Omega_b f_{\rm diff})^2}, \tag{23}$$

For the widely used F parameter, if the $\sqrt{S}-F$ relation is in the linear region, because the factor 0.979 coincidentally close to 1, we have:

$$F^2 \sim S \sim \frac{1}{H_0^3}\frac{\overline{\sigma^2}_{\rm halo}}{l}\frac{(64\pi G m_p)^2}{c(21\Omega_b f_{\rm diff})^2}, \tag{24}$$

where we confirm the anti-correlation between F and H_0 reported in Baptista et al. (2024). More specifically, we observe that $F \sim H_0^{-3/2}$. By adopting fiducial values for all parameters as in Eq. 14, and $\sqrt{\overline{\sigma^2}_{\rm halo}} \sim 130{\rm pc/cm^3}$, we provide a helpful relation:

$$F \simeq 185.75\left(\frac{H_0}{\rm km/Mpc\cdot s}\right)^{-3/2}. \tag{25}$$

This is in good qualitative agreement with Baptista et al. (2024, Figure 5), as shown in Fig. 3. The main discrepancy results from the different analyses used: Baptista et al. (2024) show their 2D marginalized distributions, when fitting 78 FRBs with a full model, including $\rm DM_{host}$. As a result, the relation between F and H_0 is affected by correlations between the different parameters. This is in contrast with our relation, which isolates the cosmological dependence of the F term, as a consequence of the halos and IGM modeling of Section 4.2.1. In our case, the underlying assumption is that halos dominate the "effective standard deviation". The actual S or F will depend on the influence of both halos and the IGM, whose detailed astrophysical modeling is left for a future work. Finally, keeping a more agnostic approach and constraining S and F directly allows a more direct comparison with Baptista et al. (2024).

4.3. *Likelihood*

Considering the two probability density functions, Eq. 8 and Eq. 9, we reach a modified convolution to calculate the total probability in the DM parameter space for each FRB:

$$p_{\rm ext}({\rm DM_{ext}}) = \frac{1}{\langle {\rm DM_{diff}}\rangle(z)}\int_0^{{\rm DM_{ext}}(1+z)} p_{\rm host}({\rm DM_{host}})\, p_\Delta\left(\frac{\rm DM_{FRB} - DM_{host,z}}{\langle {\rm DM_{diff}}\rangle(z)}\right) {\rm dDM_{host}}\,, \tag{26}$$

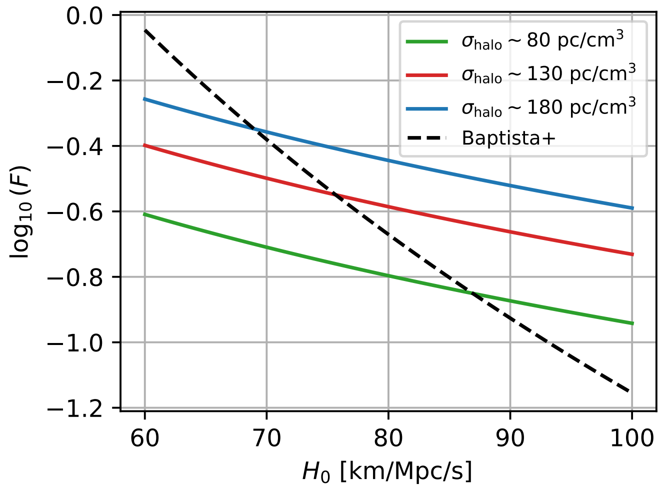

Figure 3. Cosmological dependence of F when choosing different value of $\sqrt{\sigma^2{}_{\rm halo}}$.

where $\mathrm{DM}_{\rm host,z} = \mathrm{DM}_{\rm host}/(1+z)$. We modify the convolution for two reasons. First, for $p_{\rm host}$ in Eq. 8, the log-normal distribution should be used for all host galaxies in their rest frames. Thus, when we calculate the total DM or $\mathrm{DM}_{\rm ext}$, $\mathrm{DM}_{\rm host}$ must be divided by the factor $(1 + z)$ due to cosmological effects. Second, the variable in $p_{\rm diff}$ in Eq. 9 is actually Δ rather than DM. In Macquart et al. (2020), they partially modified the convolution in their source code, which is slightly different from the equation they used in their paper. We clarify the equations here, to help reproducibility and ease of usage in future research. During the writing of this paper, Zhang et al. (2025a) also found this modification independently.

For all our well-localized FRB observations, the likelihood in DM parameter space is:

$$\mathcal{L}(\mathbf{DM}_{\rm ext}|\mathbf{H}) = \prod_{i=1}^{N_{\rm FRB}} p_{\rm ext,i}(\mathrm{DM}_{\rm ext,i}|\mathbf{H}). \tag{27}$$

$\mathbf{DM}$ represents the FRB dataset, and $\mathbf{H}$ describes the cosmological parameter space. For example, $\mathbf{H} = \{S, H_0\Omega_b f_{\rm diff}, \sigma_{\rm host}, \mu_{\rm host}\}$.

For arbitrary H priors, the posterior can then be written as:

$$p(\mathbf{H}|\mathbf{DM}_{\rm ext}) = \mathcal{L}(\mathbf{DM}_{\rm ext}|\mathbf{H})p(\mathbf{H}) \tag{28}$$

In this project, we consider uniform priors for $\mathbf{H}$, and the posterior can be simplified as:

$$p(\mathbf{H}|\mathbf{DM}_{\rm ext}) \propto \mathcal{L}(\mathbf{DM}_{\rm ext}|\mathbf{H}). \tag{29}$$

The detailed derivation of the likelihood in this section can be found in Appendix A.

5. RESULTS

In order to show the effect of a more accurate $\sigma_{\rm diff}$ $[\sigma_\Delta(S, z)]$, we utilize a Markov Chain Monte Carlo (MCMC) approach to search the parameter space $\mathbf{H}$. We first sample for our $\sigma_{\rm diff}$ $[\sigma_\Delta(S, z)]$ case. Then, for comparison, we also show the previous $\sigma_{\rm diff} \sim F/\sqrt{z}$ with the same dataset, as well as with all FRBs. We show the prior ranges for each parameter in Table 1. For $\exp(\mu)$, we choose a wide range from 10 to 300 as the median value of $\mathrm{DM}_{\rm host}$. For $\sigma_{\rm host}$, we first chose the same range as Macquart et al. (2020), but then lowered the maximum limit to save computational time, since it was not affecting the results. $\mathcal{U}[1.0, 5.0]$ is the prior for $H_0\Omega_b f_{\rm diff}$. This is a wide range based on the fiducial value 2.78 when taking $H_0 = 67.66$ km/s/Mpc, $\Omega_b = 0.04897$ (Planck Collaboration et al. 2020), and $f_{\rm diff} = 0.84$ (Li et al. 2020; Zhang et al. 2025b). As for F, this is $\mathcal{U}[0.01, 0.5]$ in Macquart et al. (2020). We choose the prior for S as $\mathcal{U}[0.008, 0.30]$, based on this range. Finally, we use a prior for F that is wider than before, i.e. $\mathcal{U}[0.01, 1.2]$, because we find a peak at larger values for the latest dataset. Note that both ranges are compatible with the physical estimates we provide in Section 4.

Table 1. Prior ranges imposed for the parameters in MCMC.

Parameters	Priors
S	$\mathcal{U}[0.008, 0.30]$
F	$\mathcal{U}[0.01, 1.2]$
$H_0\Omega_b f_{\rm diff}$	$\mathcal{U}[1.0, 5.0]$
$\sigma_{\rm host}$	$\mathcal{U}[0.2, 1.4]$
$\exp(\mu)$	$\mathcal{U}[10, 300]$

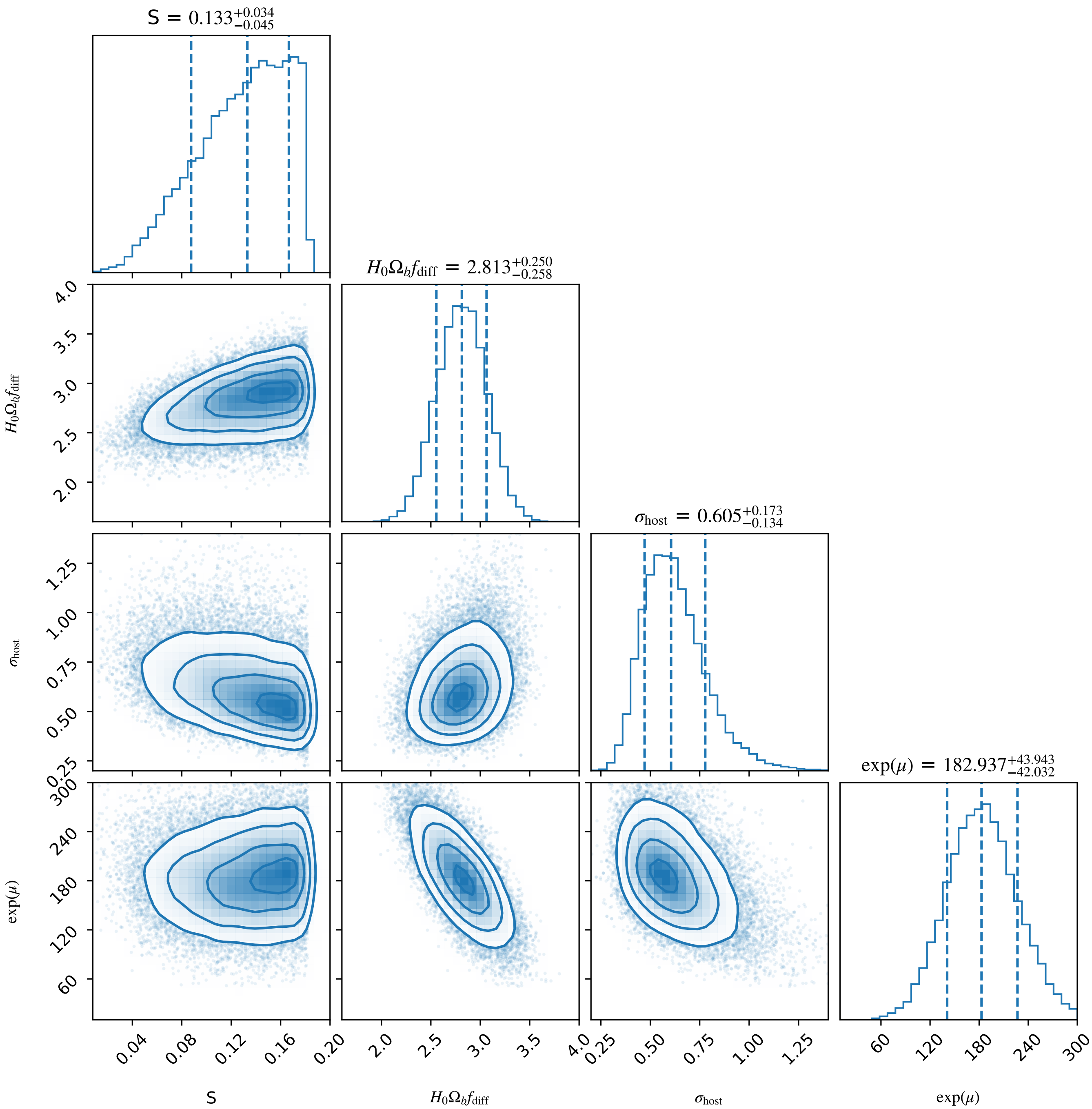

Figure 4. MCMC contour plot with our $\sigma_{\rm diff}$ correction

5.1. *A more accurate* $\sigma_{\rm diff}(\sigma_\Delta)$*, where* $\sigma_\Delta = \sigma_\Delta(S, z)$

First, we show our constraints for parameters $\mathbf{H} = \{S, H_0\Omega_b f_{\rm diff}, \sigma_{\rm host}, \mu_{\rm host}\}$ when considering a more accurate $\sigma_{\rm diff}\,[\sigma_\Delta(S,z)]$ and a modified convolution in the likelihood. We assume that $f_{\rm diff}$ is a constant. The three factors in $H_0\Omega_b f_{\rm diff}$ are always bundled and we can only constrain the product. The result of our MCMC inference is shown in Fig. 4. Note that the prior we choose for S is actually $\mathcal{U}[0.008, 0.30]$. The maximum value for S in Fig. 4 is much smaller than 0.30. The maximum is caused by the rapid growth of $\sigma_{\rm diff}$ for FRBs with small redshift. In our preliminary MCMC runs, we excluded more low-redshift FRBs and confirmed that the redshift cut of $z \geq 0.25$ is sufficient for the posterior distribution to converge to a peak value for S and also utilize the most data.

In Fig. 4, we obtain $S = 0.133^{+0.034}_{-0.045}$ and $H_0\Omega_b f_{\rm diff} = 2.813^{+0.250}_{-0.258}$ km/s/Mpc for the diffuse electron term. Also, we have $\sigma_{\rm host} = 0.605^{+0.173}_{-0.134}$ and $\exp(\mu) = 182.937^{+43.943}_{-42.032}$ pc/cm^3 for the host galaxy term. The lower and upper boundaries show the 68% confidence level. We list the results in Table 2. If we combine the CMB (Planck Collaboration et al. 2020) measurement $\Omega_b h^2 = 0.0224$ and take $f_{\rm diff} = 0.84$ (based on some earlier results including Shull et al. (2012) ($f_{\rm diff} = 0.82$), Li et al. (2020) ($f_{\rm diff} = 0.84$), Cordes et al. (2022) ($f_{\rm diff} = 0.85$), Fukugita et al. (1998) ($f_{\rm diff} = 0.83$), Zhang et al. (2025b) ($f_{\rm diff} = 0.84$)), we can obtain the $H_0 = 66.889^{+6.754}_{-5.459}$ km/s/Mpc. For the parameter S, although it differs from the previously widely used parameter F, we use Eq. 17 to estimate the equivalent F when considering that $\sigma_\Delta(S,z) \sim \widetilde{F}/\sqrt{z}$ is still linear with $\sigma_{\rm diff}$. The result shows the equivalent $F = 0.357^{+0.043}_{-0.067}$. This is consistent with the 5 FRBs "golden sample" result in Macquart et al. (2020).

Recall that for the linear range for $\sigma_{\rm diff} - \sigma_\Delta$, where F parameterization is valid in Eq. 18, we have:

$$\sigma_{\rm diff} \sim \frac{F}{\sqrt{z}} \lesssim 0.6 \tag{30}$$

Combining with the $F = 0.357^{+0.043}_{-0.067}$ constraint, the F parameter actually works only for

$$z \gtrsim 0.354 \tag{31}$$

Moreover, $\widetilde{F}$ or F are approximated from S when $z \ll 1$ (see Eq. 16 or Macquart et al. (2020)). Thus the F parameterization is plausible only under conflicting assumptions. For a rigorous estimation, the F parameter should be used for

$$0.354 \lesssim z < 1. \tag{32}$$

5.2. *A comparison with* $\sigma_{\rm diff} \sim F z^{-1/2}$

To ensure that the differences are due to the more accurate treatment to calculate $\sigma_{\rm diff}$ rather than a dataset bias, we also run an MCMC with the widely used $\sigma_{\rm diff} \sim F z^{-1/2}$ approximation, taking the same dataset while dropping the small-redshift samples. The result in Fig. 5 is more similar to the 5 FRBs "golden sample" result in Macquart et al. (2020). However, the $H_0\Omega_b f_{\rm diff}$ is much larger, corresponding to a very small Hubble constant $H_0 = 57.506^{+8.794}_{-7.209}$ km/s/Mpc if taking $\Omega_b h^2 = 0.0224$ (Planck Collaboration et al. 2020) and $f_{\rm diff} = 0.84$ (Li et al. 2020; Zhang et al. 2025b). In this method, $\sigma_{\rm diff} \sim F/\sqrt{z} \sim 1.252$ is much larger than the $\sigma_{\rm diff} - \sigma_\Delta$ linear region, which cause errors in F and $H_0\Omega_b f_{\rm diff}$.

In Fig. 6, we also show the result when we take Macquart et al. (2020)'s original $\sigma_{\rm diff} \sim F z^{-1/2}$ approximation and the entire FRB sample without dropping any low-redshift FRBs except FRB 20190520B and FRB 20220831A. In this case, F exhibits rapid growth and gets cut off. When we slightly drop some FRBs with very small redshifts, we get closer to the peak of F but also gain a larger $H_0\Omega_b f_{\rm diff}$, and finally get the result in Fig. 5 when dropping FRBs with $z < 0.25$. This also implies that $\sigma_{\rm diff} \sim F z^{-1/2}$ and $p_{\rm diff}(\Delta)$ fail to describe the PDF in the nearby universe. The limit in $\sigma_\Delta(S,z)$ actually provides a way to estimate the redshift range ($0.354 \lesssim z < 1$) that $p_{\rm diff}$ is accurate and where $\sigma_{\rm diff} \sim F z^{-1/2}$ is useful (when $\sigma_\Delta - \sigma_{\rm diff}$ is linear).

6. SUMMARY AND DISCUSSION

In this paper, we write down a clearer form for the FRB DM likelihood used to obtain cosmological constraints and discuss the effect of an accurate approach to derive $\sigma_{\rm diff}$ in $p_{\rm diff}$. More specifically, by exploiting the actual PDF of $\mathrm{DM}_{\rm diff}$, we find the relation of its true standard deviation with the effective $\sigma_{\rm diff}$ used in the literature $\sigma_{\rm diff} = \sigma_{\rm diff}\,[\sigma_\Delta(S,z)]$. We use MCMC to perform parameter estimation for $\mathbf{H} = \{S, H_0\Omega_b f_{\rm diff}, \sigma_{\rm host}, \mu_{\rm host}\}$ and investigate the performance of cosmological constraints with an improved physical modeling. Additionally, we find a suitable redshift range for $p_{\rm diff}$. In summary, we reach the following conclusions:

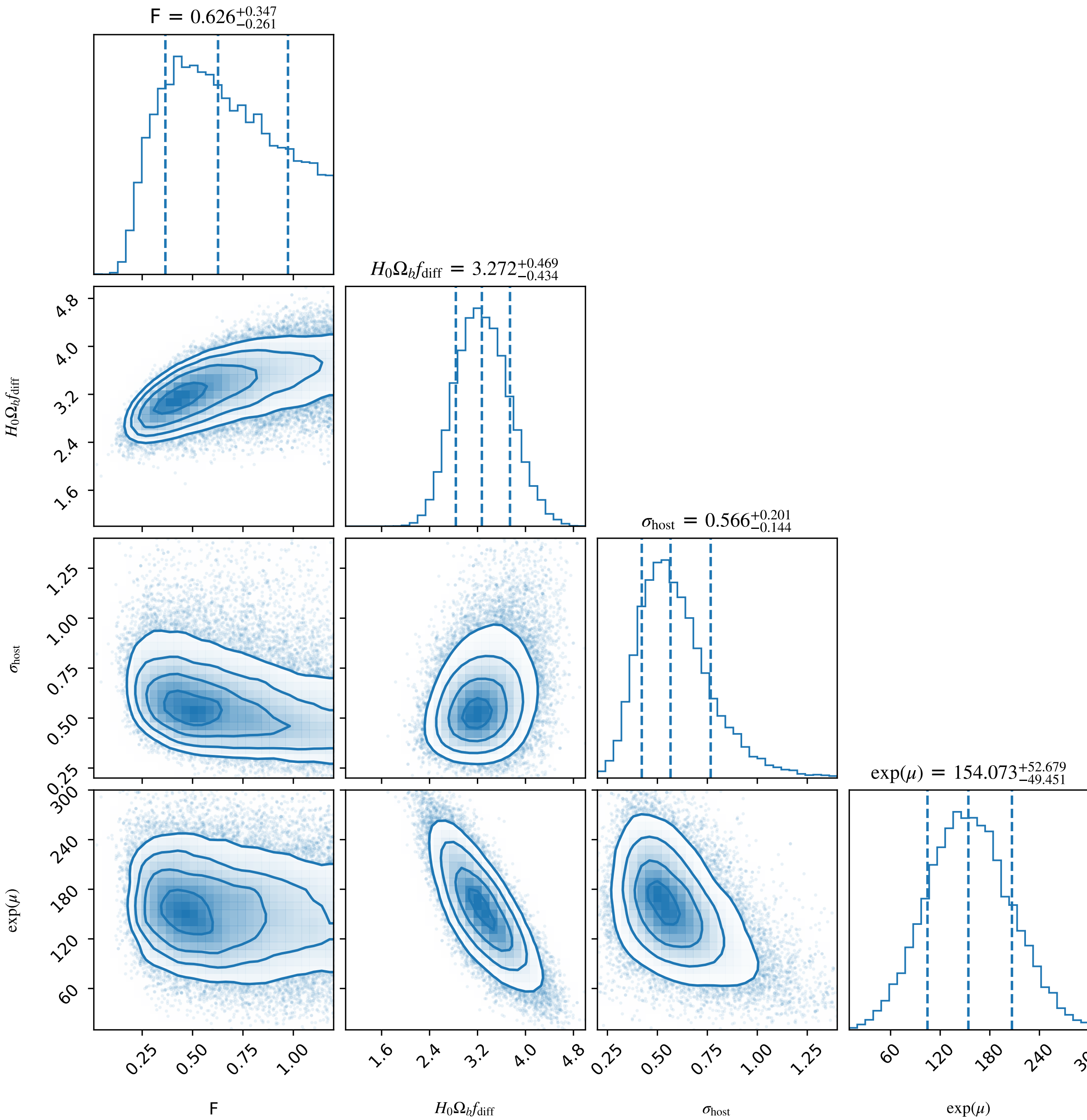

Figure 5. Macquart's $\sigma_{\rm diff} = F/\sqrt{z}$ with FRBs $z \geq 0.25$

- $\sigma_{\rm diff}$ in $p_{\rm diff}(\Delta)$ is not the true standard deviation of the variable Δ. Only when the standard deviation is not too large or the redshift is not too small, can σ_Δ and $\sigma_{\rm diff}$ take a linear relation and $\sigma_{\rm diff}$ serve as an "effective standard deviation". From our MCMC result combining the equivalent $F \sim 0.357^{+0.043}_{-0.067}$, with the linear limit $\sigma_{\rm diff} \sim F/\sqrt{z} \lesssim 0.60$, we conclude that only for $z \gtrsim 0.354$, $\sigma_{\rm diff} - \sigma_\Delta$ has a linear relation. However, only when $z \ll 1$ one can approximate $\sqrt{S} \sim F$ and have $\sigma_{\rm diff} \sim \sigma_\Delta \propto \sqrt{D_c}/\langle {\rm DM_{diff}} \rangle \propto \widetilde{F}/\sqrt{z}$. This reveals that the widely used F parameter in $\sigma_{\rm diff} \sim F/\sqrt{z}$ only works under two contrived and contradictory assumptions. Otherwise, we must take the accurate form $\sigma_{\rm diff}\left[\sigma_\Delta(S, z)\right]$.

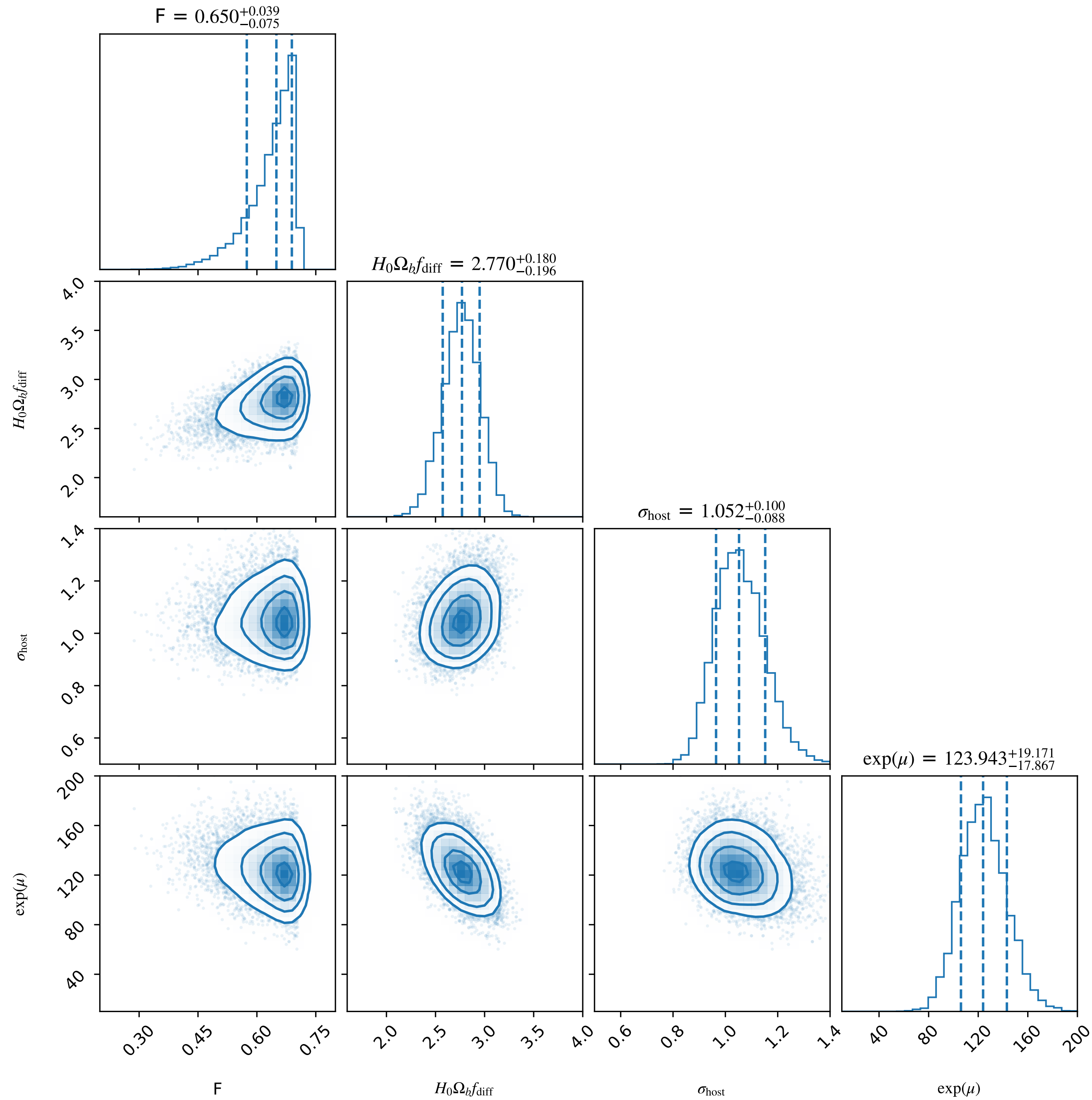

Figure 6. Macquart's $\sigma_{\rm diff} = F/\sqrt{z}$ with 115 localized FRBs

- In the non-linear regime for $\log(\sigma_\Delta) - \log(\sigma_{\rm diff})$, σ_Δ has a maximum limit. When σ_Δ approaches the maximum value, $\sigma_{\rm diff}$ diverges logarithmically. Very large σ_Δ values are associated with very small redshifts, which means that $p_{\rm diff}(\Delta)$ may not work in the low-redshift regime, which reminds us that $\sigma_{\rm diff}$ cannot be an "effective standard deviation" there. In the future, $p_{\rm diff}$ still needs to be revisited in more detail, especially in the low-redshift regime. One way is to consider the halo and IGM components at different redshifts. The α and β in $p_{\rm diff}(\Delta)$ may need to be modified when we also consider the IGM component in the diffuse electron term. AGN feedback will also affect the gas density profile in the halos and influence α and β. Another possible approach

Table 2. Results for $\mathbf{H} = \{S$ (or F if Macquart et al. (2020) original approximation), $H_0\Omega_b f_{\rm diff}, \sigma_{\rm host}, \mu_{\rm host}\}$ with 68% confidence interval. We show the results of our correction using MCMC. We also show Macquart et al. (2020)'s original method using the same FRB samples and 115 localized FRBs for comparison. We also show the corresponding F (or S) according to Eq. 17 to easily show their magnitudes. The H_0 column is calculated from $H_0\Omega_b f_{\rm diff}$ using $\Omega_b h^2 = 0.0224$ (Planck Collaboration et al. 2020) and $f_{\rm diff} = 0.84$ (Li et al. 2020; Zhang et al. 2025b).

Method	**Data**	S	F	$H_0\Omega_b f_{\rm diff}$ (km/s/Mpc)	$\sigma_{\rm host}$	$\exp(\mu)$ (pc/cm^3)	H_0 (km/s/Mpc)
$\sigma_{\rm diff}(S,z)$	$z \geq 0.25$	$0.133^{+0.034}_{-0.045}$	$\sim 0.357^{+0.043}_{-0.067}$	$2.813^{+0.250}_{-0.258}$	$0.605^{+0.173}_{-0.134}$	$182.937^{+43.943}_{-42.032}$	$66.889^{+6.754}_{-5.459}$
$\sigma_{\rm diff} = F/\sqrt{z}$	$z \geq 0.25$	$\sim 0.409^{+0.579}_{-0.270}$	$0.626^{+0.347}_{-0.261}$	$3.272^{+0.469}_{-0.434}$	$0.566^{+0.201}_{-0.144}$	$154.072^{+52.679}_{-49.451}$	$57.506^{+8.794}_{-7.209}$
$\sigma_{\rm diff} = F/\sqrt{z}$	115 FRBs samples	$> 0.441^{+0.055}_{-0.096}$	$> 0.650^{+0.039}_{-0.075}$	$> 2.770^{+0.180}_{-0.196}$	$1.052^{+0.100}_{-0.088}$	$123.943^{+19.171}_{-17.867}$	$< 67.928^{+5.172}_{-4.145}$

is to directly take the PDF for $\mathrm{DM}_{\rm diff}$ rather than for Δ. This intrinsic PDF will have a convergent standard deviation. However, $p_{\rm diff}$ will require a wider search range to find C_0, which will cause other numerical problems.

- With our more accurate parameter consideration, S, $\widetilde{F}$, or F actually acquire a physical meaning (see Eq. 14). For the first time we provide a physical explanation for the correlation observed in (Baptista et al. 2024). This allows us to propose a new approach to constrain cosmological parameters. These parameters represent the combination of some cosmological parameters, halo baryon fluctuations, and the mean observed halo path from the FRB perspective. If we understand more about the halo density profiles and baryon distributions, these parameters provide another way to measure $1/S \propto H_0^3\Omega_b^2 f_{\rm diff}^2$ and to constrain cosmological parameters.

- With our new $\sigma_{\rm diff}$ $[\sigma_\Delta(S,z)]$, we obtain the constraints $S = 0.133^{+0.034}_{-0.045}$, $H_0\Omega_b f_{\rm diff} = 2.813^{+0.250}_{-0.258}$ km/s/Mpc, and $\widetilde{\mathrm{DM}}_{\rm host} = \exp(\mu) = 182.937^{+43.943}_{-42.032}$ pc/cm^3. When combined with the Planck18 results (Planck Collaboration et al. 2020) and $f_{\rm diff} = 0.84$, we constrain the Hubble constant to $H_0 = 66.889^{+6.754}_{-5.459}$ km/s/Mpc. Many previous cosmological constraints from other methods are within this range. One can expect FRBs to become an accurate probe to constrain cosmological parameters if, in the future, we have more localized FRBs and understand more about their host galaxies as well as the intervening halos.

We thank J. X. Prochaska for the informative discussion to allow us know about the details of the treatment in Macquart et al. (2020). We also acknowledge some helpful suggestions from Carl-Johan Haster. JZ thanks the helpful discussion with Yuanhong Qu, Zi-Liang Zhang, Yihan Wang and Rui-Chong Hu. JZ and BZ's work is supported by the Nevada Center for Astrophysics, NASA 80NSSC23M0104 and a Top Tier Doctoral Graduate Research Assistantship (TTDGRA) at University of Nevada, Las Vegas.

Software: NumPy (Harris et al. 2020), astropy (Astropy Collaboration et al. 2013, 2018), Matplotlib (Hunter 2007), SciPy (Virtanen et al. 2020), pandas (Wes McKinney 2010; Team 2023), emcee (Foreman-Mackey et al. 2013), PyGEDM (Price et al. 2021). The core pipeline and reproduction codes for the cosmological analysis in this work are publicly available on GitHub (https://github.com/MariosNT/FRB_GW_association_cosmo) and permanently archived on Zenodo via doi:10.5281/zenodo.20282512 (Zhuge & Kalomenopoulos 2026).

APPENDIX

A. LIKELIHOOD CALCULATION FOR DM OF FRBS

A.1. *2 PDFs case*

In this section, we provide a detailed derivation of Eq. 26 that calculates the likelihood of the observed DM ($\mathrm{DM}_{\rm obs}$) of a given FRB with redshift z. In statistics, assume the sum of two independent, random variables X, Y with probability density functions (PDF) $p_X(x)$, $p_Y(y)$. The random variable Z calculated by $Z = X + Y$, would have a

PDF given from the convolution of p_X and p_Y (e.g. Blitzstein & Hwang 2019):

$$p_Z(z) = (p_X * p_Y)(z) = \int_a^b p_X(\tau)p_Y(z-\tau)d\tau. \tag{A1}$$

The upper and lower limits may be adjusted according to the range of the variables.

For an FRB, we subtract the MW term from its $\mathrm{DM_{obs}}$ and get extragalactic DM ($\mathrm{DM_{ext}}$). The remaining terms include the diffuse medium term and the host environment term:

$$\mathrm{DM_{ext}} = \mathrm{DM_{diff}} + \mathrm{DM_{host,z}}. \tag{A2}$$

Note that the DM that we actually measure is in the Earth frame, meaning that a redshift correction is applied to the $\mathrm{DM_{host,z}}$, i.e. $\mathrm{DM_{host,z}} = \mathrm{DM_{host}}/(1+z)$, where $z = z_{\mathrm{FRB}}$. This means that in reality, we want to calculate the PDF of:

$$\mathrm{DM_{ext}} = \mathrm{DM_{diff}} + \mathrm{DM_{host,z}} = \mathrm{DM_{diff}} + \frac{\mathrm{DM_{host}}}{1+z}. \tag{A3}$$

At the same time, one must be careful because in Eq. 9, $p_{\mathrm{diff}}(\Delta = \mathrm{DM}/\langle \mathrm{DM_{diff}}\rangle)$ is not in the same variable space as $p_{\mathrm{host}}(\mathrm{DM})$. This means that a change of variables is required for both distributions. Demanding the conservation of probability, we have:

$$p_{\mathrm{DM_{host,z}}}(\mathrm{DM_{host,z}})\,\mathrm{dDM_{host,z}} = p_{\mathrm{host}}(\mathrm{DM_{host}})\,\mathrm{dDM_{host}} \quad \Rightarrow \quad p_{\mathrm{DM_{host,z}}}(\mathrm{DM_{host,z}}) = p_{\mathrm{host}}(\mathrm{DM_{host}})(1+z) \tag{A4}$$

$$p_{\mathrm{DM_{diff}}}(\mathrm{DM_{diff}})\,\mathrm{dDM_{diff}} = p_\Delta(\Delta)\,\mathrm{d}\Delta \quad \Rightarrow \quad p_{\mathrm{DM_{diff}}}(\mathrm{DM_{diff}}) = p_\Delta(\Delta)/\langle \mathrm{DM_{diff}}\rangle. \tag{A5}$$

Then, for convolution in the DM space, for an individual FRB $\mathrm{DM_{FRB}} = \mathrm{DM_{host,z}} + \mathrm{DM_{IGM}}$, we have

$$\begin{aligned} p(\mathrm{DM_{FRB}}) = (p_{\mathrm{DM_{host,z}}} * p_{\mathrm{DM_{diff}}}) &= \int_0^{\mathrm{DM_{FRB}}} p_{\mathrm{DM_{host,z}}}(\mathrm{DM_{host,z}})p_{\mathrm{DM_{IGM}}}(\mathrm{DM_{FRB}} - \mathrm{DM_{host,z}})\mathrm{dDM_{host,z}} \\ &= \int_0^{\mathrm{DM_{FRB}}(1+z)} p_{\mathrm{host}}(\mathrm{DM_{host}})p_\Delta\left(\frac{\mathrm{DM_{FRB}} - \mathrm{DM_{host,z}}}{\langle \mathrm{DM_{diff}}\rangle(z)}\right)\frac{\mathrm{dDM_{host}}}{\langle \mathrm{DM_{diff}}\rangle}, \end{aligned} \tag{A6}$$

where we have used Eq. (A4, A5) in the second step. More clearly, one has

$$\boxed{p(\mathrm{DM_{FRB}}) = \frac{1}{\langle \mathrm{DM_{diff}}\rangle}\int_0^{\mathrm{DM_{FRB}}(1+z)} p_{\mathrm{host}}(\mathrm{DM_{host}})p_\Delta\left(\frac{\mathrm{DM_{FRB}} - \mathrm{DM_{host,z}}}{\langle \mathrm{DM_{diff}}\rangle}\right)\mathrm{dDM_{host}}} \tag{A7}$$

Alternatively, if one does convolution in the Δ space, one has

$$\mathrm{DM_{FRB}} = \mathrm{DM_{host,z}} + \mathrm{DM_{diff}} = \mathrm{DM_{host,z}} + \Delta\cdot\langle \mathrm{DM_{diff}}\rangle \Rightarrow \mathrm{DM_{host}}/(1+z) = \mathrm{DM_{FRB}} - \Delta\cdot\langle \mathrm{DM_{diff}}\rangle. \tag{A8}$$

The PDF becomes

$$\begin{aligned} p(\mathrm{DM_{FRB}}) = (p_{\mathrm{DM_{host,z}}} * p_{\mathrm{DM_{diff}}}) &= \int_0^{\mathrm{DM_{FRB}}} p_{\mathrm{DM_{host,z}}}(\mathrm{DM_{FRB}} - \mathrm{DM_{diff}})p_{\mathrm{DM_{diff}}}(\mathrm{DM_{diff}})d\mathrm{DM_{diff}} \\ &= \int_0^{\mathrm{DM_{FRB}}/\langle \mathrm{DM_{diff}}\rangle(z)} p_{\mathrm{host,z}}(\mathrm{DM_{FRB}} - \Delta\cdot\langle \mathrm{DM_{diff}}\rangle)p_\Delta(\Delta)d\Delta \\ &= \int_0^{\mathrm{DM_{FRB}}/\langle \mathrm{DM_{diff}}\rangle(z)} (1+z)p_{\mathrm{host}}\left((1+z)\cdot(\mathrm{DM_{FRB}} - \Delta\cdot\langle \mathrm{DM_{diff}}\rangle)\right)p_\Delta(\Delta)d\Delta, \end{aligned} \tag{A9}$$

which finally gives

$$\boxed{p(\mathrm{DM_{FRB}}) = (1+z)\int_0^{\mathrm{DM_{FRB}}/\langle \mathrm{DM_{diff}}\rangle(z)} p_{\mathrm{host}}\left[(1+z)\cdot(\mathrm{DM_{FRB}} - \Delta\cdot\langle \mathrm{DM_{diff}}\rangle)\right]p_\Delta(\Delta)d\Delta} \tag{A10}$$

Obviously Eq. A10 and Eq. A7 are equivalent.

For multiple, well-localized FRB observations, one has

$$\mathcal{L}(\mathbf{DM}|\mathbf{H}) = \prod_{i=1}^{N_{\rm FRB}} p_{\rm DM_{FRB,i}}(\rm DM_{FRB,i}|\mathbf{H}). \tag{A11}$$

DM represents the FRBs dataset, and **H** describes the parameter space.

The final posterior can then be written as:

$$p(\mathbf{H}|\mathbf{DM}) \propto \mathcal{L}(\mathbf{DM}|\mathbf{H}) \cdot p(\mathbf{H}). \tag{A12}$$

A.2. *Likelihood based on conditional probabilities*

In the previous subsection, we derived the convolution for FRBs PDFs used in in this project, but we have skipped some steps. The combined PDF is actually a conditional probability. In this subsection, we derive it mathematically.

To calculate the probability of $Z = X + Y$, we start by calculating the joint probability $p(Z, X, Y)$:

$$p(Z, X, Y) = p(Z|X, Y)p(X, Y) = p(Z|X, Y)p(X|Y)p(Y) = p(Z|X, Y)p(X)p(Y), \tag{A13}$$

where in the first step, we used the definition of the conditional probability, and in the second, we used the assumption that X, Y are independent.

To get $p(Z)$ we marginalise the probability over X, Y:

$$p(Z) = \int dX \int dY \; p(Z, X, Y) = \int dX \int dY \; p(Z|X, Y)p(X)p(Y). \tag{A14}$$

Since $Z = X + Y$, the variables are not independent and if we know X, Y, then there is only one possible value of Z, i.e.

$$p(Z|X, Y) = \delta\left(Z - (X + Y)\right), \tag{A15}$$

where δ is the Dirac δ-function.

Inserting this in the integral, we get:

$$p(Z) = \int dX \int dY \; \delta\left(Z - (X + Y)\right) p(X)p(Y) = \int dX \; p(X)p(Z - X), \tag{A16}$$

so we end up with the convolution as in Eq. A1. For $Z = \rm DM_{FRB}$, $X = \rm DM_{host,z}$ and $Y = \rm DM_{diff}$, this yields:

$$p(\rm DM_{FRB}) = \int_0^{\rm DM_{FRB}} p_{\rm DM_{host,z}}(\rm DM_{host,z}) p_{\rm DM_{diff}}(\rm DM_{FRB} - DM_{host,z}) d\rm DM_{host,z} \tag{A17}$$

which is the same as Eq. A6, and one can then follow a similar procedure as above.

A.3. *The case of three PDFs*

In reality, FRB DM is not just composed of the MW, diffuse medium, and host galaxy terms. For example, Kalita et al. (2024) also considered a Gaussian distribution for the Milky Way halo component. We consider one extra term: the third component in the external DM term, i.e. $\rm DM_{src}$, which refers to the DM contribution from the immediate environment of the FRB source. Then one defines the total host component as $\rm DM_{hosts}$:

$$\rm DM_{hosts} = DM_{host} + DM_{src} \tag{A18}$$

It is easy to get the probability for the host term, i.e.

$$p_{\rm hosts}(\rm DM_{hosts}) = \int_0^{\rm DM_{hosts}} p_{\rm host}(\rm DM_{hosts} - DM_{src}) p_{\rm src}(\rm DM_{src}) \, dDM_{src} \tag{A19}$$

One can simply replace $\rm DM_{host}$ with $\rm DM_{hosts}$ in Eq. A7 to obtain

$$p(\rm DM_{FRB}) = \frac{1}{\langle \rm DM_{diff}\rangle(z)} \int_0^{\rm DM_{FRB}(1+z)} p_\Delta \left(\frac{\rm DM_{FRB} - DM_{hosts,z}}{\langle \rm DM_{diff}\rangle(z)}\right) \int_0^{\rm DM_{hosts}} p_{\rm host}(\rm DM_{hosts} - DM_{src}) p_{\rm src}(\rm DM_{src}) \, dDM_{src} \, dDM_{hosts} \tag{A20}$$

It is straightforward to show that this is equivalent to

$$p(\mathrm{DM_{FRB}}) = \frac{1}{\langle \mathrm{DM_{diff}}\rangle(z)} \int_0^{\mathrm{DM_{host}}=\mathrm{DM_{FRB}}(1+z)} \int_0^{\mathrm{DM_{src}}=\mathrm{DM_{FRB}}(1+z)-\mathrm{DM_{host}}} p_\Delta\left(\frac{\mathrm{DM_{FRB}}-\mathrm{DM_{host,z}}-\mathrm{DM_{src,z}}}{\langle \mathrm{DM_{diff}}\rangle(z)}\right) p_{\mathrm{host}}(\mathrm{DM_{host}}) \times p_{\mathrm{src}}(\mathrm{DM_{src}})\, \mathrm{dDM_{src}}\, \mathrm{dDM_{host}}\,. \tag{A21}$$

This is just an example for the three PDFs. One can modify the treatment to include other DM contributions as required.

B. FRB DATA

Table 3. Well localized FRB samples

FRB	z	gl (deg)	gb (deg)	$\mathrm{DM_{obs}}$ ($\mathrm{pc\,cm^{-3}}$)	$\mathrm{DM_{MW,ISM}}$(NE2001) ($\mathrm{pc\,cm^{-3}}$)	$\mathrm{DM_{MW,ISM}}$(YMW16) ($\mathrm{pc\,cm^{-3}}$)	Ref.
FRB 20121102A	0.19273	174.89	-0.23	557.0	188.42	287.07	1, 40
FRB 20171020A	0.00867	29.3	-51.3	114.1	38.37	25.84	36, 13
FRB 20180301A	0.3304	204.412	-6.481	522.0	150.73	252.56	24
FRB 20180814A	0.068	136.46	16.58	190.9	87.83	108.41	37
FRB 20180916B	0.0338	129.71	3.73	348.76	198.91	324.82	5, 41, 34
FRB 20180924B	0.3214	0.7424	-49.4147	361.75	40.5	27.65	3, 6, 23, 11, 20, 42
FRB 20181030A	0.00385	133.4	40.9	103.5	40.35	32.24	27
FRB 20181112A	0.4755	342.5995	-47.6988	589.0	41.72	29.03	4, 6, 23, 20, 42
FRB 20181220A	0.02746	105.24	-10.73	209.4	125.85	122.13	28
FRB 20181223C	0.03024	207.75	79.51	112.5	19.93	19.15	28
FRB 20190102C	0.29	312.6537	-33.4931	364.55	57.4	43.28	6, 23, 20, 42
FRB 20190110C	0.12244	65.6	42.1	221.6	37.07	29.95	33
FRB 20190303A	0.064	97.5	65.7	222.4	29.67	21.83	37
FRB 20190418A	0.07132	179.3	-22.93	184.5	70.11	85.6	28
FRB 20190425A	0.03122	42.06	33.02	128.2	48.8	38.81	28
FRB 20190520B	0.241	359.67	29.91	1204.7	60.21	50.23	9, 11
FRB 20190523A	0.66	117.03	44.0	760.8	37.18	29.88	2
FRB 20190608B	0.11778	53.2088	-48.5296	339.5	37.27	26.62	6, 23, 11, 20, 42
FRB 20190611B	0.3778	312.9352	-33.2818	322.4	57.83	43.67	32, 6, 20, 42
FRB 20190614D	0.6	136.3	16.5	959.2	88.0	109.06	35
FRB 20190711A	0.522	310.9081	-33.902	592.0	56.49	42.61	32, 6, 20, 42
FRB 20190714A	0.2365	289.6972	48.9359	504.7	38.49	31.16	32, 20, 42
FRB 20191001A	0.23	341.2267	-44.9039	507.0	44.17	31.08	32, 20, 42
FRB 20191106C	0.10775	105.7	73.2	332.2	25.01	20.54	33
FRB 20191228A	0.2432	20.5553	-64.9245	297.0	32.95	19.92	24, 20, 42
FRB 20200120E	0.00014	142.19	41.22	87.82	40.67	32.23	26, 31
FRB 20200223B	0.06024	118.1	-33.9	201.8	45.53	36.99	33
FRB 20200430A	0.1608	17.1396	52.503	380.1	27.18	26.08	32, 20, 42
FRB 20200906A	0.3688	202.257	-49.9989	577.8	35.84	37.87	24, 20, 42

Table 3 *continued on next page*

Table 3 *(continued)*

FRB	z	gl (deg)	gb (deg)	DM_{obs} ($pc\,cm^{-3}$)	$DM_{MW,ISM}$(NE2001) ($pc\,cm^{-3}$)	$DM_{MW,ISM}$(YMW16) ($pc\,cm^{-3}$)	Ref.
FRB 20201123A	0.0507	340.23	-9.68	433.55	251.66	162.66	7
FRB 20201124A	0.098	177.6	-8.5	413.52	140.13	196.69	8
FRB 20210117A	0.214	45.9175	-57.6464	729.2	34.38	23.1	25, 11, 20, 42
FRB 20210320C	0.28	318.8729	45.3081	384.6	39.29	30.39	11, 20, 42
FRB 20210405I	0.066	338.19	-4.59	565.17	516.78	349.21	16
FRB 20210410D	0.1415	312.32	-34.13	578.78	56.19	42.24	12, 11
FRB 20210603A	0.1772	119.71	-41.58	500.147	39.53	30.79	18
FRB 20210807D	0.12927	39.8612	-14.8775	251.9	121.17	93.66	11, 20
FRB 20211127I	0.046946	312.0214	43.5427	234.83	42.47	31.46	11, 31, 20, 42
FRB 20211203C	0.3439	314.5185	30.4361	636.2	63.73	48.38	11, 20, 42
FRB 20211212A	0.0707	244.0081	47.3154	200.0	38.75	27.46	11, 20, 42
FRB 20220105A	0.2785	18.555	74.808	583.0	22.04	20.63	11, 20, 42
FRB 20220204A	0.4012	102.26	27.06	612.2	52.84	48.7	15, 38, 30
FRB 20220207C	0.0433	106.94	18.39	262.3	76.1	83.27	39, 15, 38, 30
FRB 20220208A	0.351	107.62	15.36	437.0	90.4	107.92	15, 38, 30
FRB 20220307B	0.2481	116.24	10.47	499.15	128.25	186.98	39, 15, 38, 30
FRB 20220310F	0.478	140.02	34.8	462.15	46.34	39.51	39, 15, 38, 30
FRB 20220319D	0.0112	129.18	9.11	110.95	139.71	210.96	39, 15, 38, 30, 19
FRB 20220330D	0.3714	134.18	42.93	468.1	38.98	30.63	15, 38, 30
FRB 20220418A	0.6213	110.75	44.47	623.45	36.65	29.54	39, 15, 38, 30
FRB 20220501C	0.381	11.1777	-71.4731	449.5	30.62	14.0	20, 38, 42
FRB 20220506D	0.3004	108.35	16.51	369.93	84.58	97.69	39, 15, 38, 30
FRB 20220509G	0.0894	100.94	25.48	269.5	55.6	52.06	39, 15, 38, 30
FRB 20220529A	0.1839	130.7877	-41.858	246.0	39.95	30.92	22
FRB 20220610A	1.015	8.8392	-70.1857	1458.1	30.96	13.58	20, 42
FRB 20220717A	0.36295	19.8352	-17.632	637.34	118.33	83.22	17
FRB 20220725A	0.1962	0.0017	-71.1863	290.1	30.73	11.58	20, 42
FRB 20220726A	0.3619	139.97	17.57	686.55	83.65	101.14	15, 38, 30
FRB 20220825A	0.2414	106.99	17.79	651.2	78.46	86.91	39, 15, 38, 30
FRB 20220831A	0.262	110.96	12.47	1146.25	110.21	147.77	30
FRB 20220912A	0.0771	347.27	48.7	219.46	32.5	28.6	10
FRB 20220914A	0.1139	104.31	26.13	631.05	54.68	51.11	15, 38, 30
FRB 20220918A	0.491	300.6851	-46.2342	643.0	40.74	28.87	20, 42
FRB 20220920A	0.1582	104.92	38.89	315.0	39.86	33.36	39, 15, 38, 30
FRB 20221012A	0.2847	101.14	26.14	442.2	54.35	50.55	39, 15, 38, 30
FRB 20221027A	0.5422	142.66	33.96	452.5	47.62	41.07	15, 38, 30
FRB 20221029A	0.975	140.39	38.01	1391.05	43.15	35.42	15, 38, 30
FRB 20221101B	0.2395	113.25	11.06	490.7	122.68	174.2	15, 38, 30
FRB 20221106A	0.2044	220.901	-50.8788	343.2	34.79	31.84	20, 42
FRB 20221113A	0.2505	139.53	16.99	411.4	86.31	105.52	38, 30

Table 3 *continued on next page*

Table 3 *(continued)*

FRB	z	gl (deg)	gb (deg)	DM_{obs} ($pc\,cm^{-3}$)	$DM_{MW,ISM}$(NE2001) ($pc\,cm^{-3}$)	$DM_{MW,ISM}$(YMW16) ($pc\,cm^{-3}$)	Ref.
FRB 20221116A	0.2764	124.47	8.71	640.6	145.05	223.48	38, 30, 20
FRB 20221219A	0.553	103.19	34.07	706.708	43.97	37.98	38, 30
FRB 20230124A	0.0939	107.55	40.25	590.574	39.13	32.36	38, 30
FRB 20230203A	0.1464	188.7125	54.087	420.1	36.26	22.95	21
FRB 20230216A	0.531	242.6	46.33	828.0	39.46	28.15	38, 30
FRB 20230222A	0.1223	204.7164	8.6957	706.1	134.2	188.08	21
FRB 20230222B	0.11	49.6176	49.9787	187.8	27.73	26.29	21
FRB 20230307A	0.2706	127.35	45.0	608.854	37.4	29.26	38, 30
FRB 20230311A	0.1918	157.7134	16.0395	364.3	92.46	115.68	21
FRB 20230501A	0.3015	112.43	11.51	532.471	118.55	165.22	38, 30
FRB 20230521B	1.354	115.65	9.97	1342.9	133.4	197.8	30
FRB 20230526A	0.157	290.171	-63.4721	316.2	31.86	21.86	20, 42
FRB 20230626A	0.327	105.68	38.34	451.2	40.21	33.85	38, 30
FRB 20230628A	0.127	135.48	42.21	344.952	39.59	31.17	38, 30
FRB 20230703A	0.1184	137.2098	67.475	291.3	26.93	20.67	21
FRB 20230708A	0.105	342.6288	-33.3877	411.51	60.33	43.99	20, 42
FRB 20230712A	0.4525	132.31	43.69	587.567	38.44	30.1	38, 30
FRB 20230718A	0.035	259.4629	-0.3666	476.67	420.65	449.99	20, 42
FRB 20230730A	0.2115	158.8166	-17.8164	312.5	85.16	97.38	21
FRB 20230814A	0.553	112.56	13.2	696.4	104.76	137.79	30
FRB 20230814B	0.5535	111.25	12.26	696.4	111.87	151.38	30
FRB 20230902A	0.3619	256.9906	-53.3387	440.1	34.14	25.53	20, 42
FRB 20230926A	0.0553	68.2353	27.484	222.8	52.62	43.72	21
FRB 20231005A	0.0713	57.1653	44.3532	189.4	33.47	28.79	21
FRB 20231011A	0.0783	127.2287	-20.943	186.3	70.35	65.69	21
FRB 20231017A	0.245	100.6098	-21.6519	344.2	64.55	55.64	21
FRB 20231025B	0.3238	93.4332	29.434	368.7	48.59	43.37	21
FRB 20231120A	0.0368	140.43	37.94	438.9	43.22	35.5	38, 30
FRB 20231123A	0.0729	199.3094	-15.7427	302.1	89.75	136.86	21
FRB 20231123B	0.2621	105.71	38.38	396.857	40.36	33.82	38, 30
FRB 20231128A	0.1079	105.6852	73.224	331.6	25.01	20.54	21
FRB 20231201A	0.1119	163.0405	-22.7702	169.4	69.95	74.72	21
FRB 20231204A	0.0644	97.6238	65.9281	221.0	29.83	21.79	21
FRB 20231206A	0.0659	161.0582	27.4819	457.7	59.14	59.29	21
FRB 20231220A	0.3355	143.29	31.69	491.2	50.27	45.17	30
FRB 20231223C	0.1059	52.3107	32.0802	165.8	47.87	38.64	21
FRB 20231226A	0.1569	236.5768	48.6458	329.9	38.09	26.69	20, 42
FRB 20231229A	0.019	135.3449	-26.4433	198.5	58.18	51.77	21
FRB 20231230A	0.0298	195.8701	-25.2387	131.4	61.58	83.27	21
FRB 20240114A	0.1306	57.73	-31.68	527.7	49.42	38.77	14, 29

Table 3 *continued on next page*

Table 3 *(continued)*

FRB	z	gl (deg)	gb (deg)	DM_{obs} ($pc\,cm^{-3}$)	$DM_{MW,ISM}$(NE2001) ($pc\,cm^{-3}$)	$DM_{MW,ISM}$(YMW16) ($pc\,cm^{-3}$)	Ref.
FRB 20240119A	0.376	112.37	43.24	483.1	37.36	30.32	30
FRB 20240123A	0.968	138.14	15.34	1462.0	94.02	119.71	30
FRB 20240201A	0.042729	222.1335	47.9692	374.5	38.62	29.14	20, 42
FRB 20240210A	0.023686	14.4396	-86.2116	283.73	28.69	17.9	20, 42
FRB 20240213A	0.1185	136.49	41.57	357.4	40.1	31.76	30
FRB 20240215A	0.21	102.29	30.17	549.5	48.29	43.11	30
FRB 20240229A	0.287	131.13	44.11	491.15	37.94	29.81	30
FRB 20240310A	0.127	291.7066	-72.2713	601.8	30.1	19.83	20, 42

Note—Reference: (1) Chatterjee et al. (2017); (2) Ravi et al. (2019); (3) Bannister et al. (2019); (4) Prochaska et al. (2019); (5) Marcote et al. (2020); (6) Macquart et al. (2020); (7) Rajwade et al. (2022); (8) Ravi et al. (2022); (9) Niu et al. (2022); (10) Ravi et al. (2023); (11) Gordon et al. (2023); (12) Caleb et al. (2023); (13) Lee-Waddell et al. (2023); (14) Kumar et al. (2024); (15) Sherman et al. (2024); (16) Driessen et al. (2024); (17) Rajwade et al. (2024); (18) Cassanelli et al. (2024); (19) Ravi et al. (2025); (20) Shannon et al. (2025); (21) FRB Collaboration et al. (2025); (22) Li et al. (2025); (23) Bhandari et al. (2020); (24) Bhandari et al. (2022); (25) Bhandari et al. (2023); (26) Bhardwaj et al. (2021a); (27) Bhardwaj et al. (2021b); (28) Bhardwaj et al. (2024); (29) Chen et al. (2025); (30) Connor et al. (2025); (31) Glowacki et al. (2023); (32) Heintz et al. (2020); (33) Ibik et al. (2024); (34) Kaur et al. (2022); (35) Law et al. (2020); (36) Mahony et al. (2018); (37) Michilli et al. (2023); (38) Sharma et al. (2024); (39) Sherman et al. (2023); (40) Tendulkar et al. (2017); (41) Tendulkar et al. (2021); (42) Scott et al. (2025)

REFERENCES

Acharya, S. K., & Beniamini, P. 2025, arXiv e-prints, arXiv:2503.08441, doi: 10.48550/arXiv.2503.08441

Arcus, W. R., Macquart, J.-P., Sammons, M. W., James, C. W., & Ekers, R. D. 2020, Monthly Notices of the Royal Astronomical Society, 501, 5319, doi: 10.1093/mnras/staa3948

Astropy Collaboration, Robitaille, T. P., Tollerud, E. J., et al. 2013, A&A, 558, A33, doi: 10.1051/0004-6361/201322068

Astropy Collaboration, Price-Whelan, A. M., Sipőcz, B. M., et al. 2018, AJ, 156, 123, doi: 10.3847/1538-3881/aabc4f

Bannister, K. W., Deller, A. T., Phillips, C., et al. 2019, Science, 365, 565, doi: 10.1126/science.aaw5903

Baptista, J., Prochaska, J. X., Mannings, A. G., et al. 2024, ApJ, 965, 57, doi: 10.3847/1538-4357/ad2705

Bhandari, S., Sadler, E. M., Prochaska, J. X., et al. 2020, The Astrophysical Journal Letters, 895, L37, doi: 10.3847/2041-8213/ab672e

Bhandari, S., Heintz, K. E., Aggarwal, K., et al. 2022, The Astronomical Journal, 163, 69, doi: 10.3847/1538-3881/ac3aec

Bhandari, S., Gordon, A. C., Scott, D. R., et al. 2023, The Astrophysical Journal, 948, 67, doi: 10.3847/1538-4357/acc178

Bhardwaj, M., Gaensler, B. M., Kaspi, V. M., et al. 2021a, The Astrophysical Journal Letters, 910, L18, doi: 10.3847/2041-8213/abeaa6

Bhardwaj, M., Kirichenko, A. Y., Michilli, D., et al. 2021b, The Astrophysical Journal Letters, 919, L24, doi: 10.3847/2041-8213/ac223b

Bhardwaj, M., Michilli, D., Kirichenko, A. Y., et al. 2024, The Astrophysical Journal Letters, 971, L51, doi: 10.3847/2041-8213/ad64d1

Blitzstein, J., & Hwang, J. 2019, Introduction to Probability Second Edition (Chapman and Hall/CRC)

Caleb, M., Driessen, L. N., Gordon, A. C., et al. 2023, MNRAS, 524, 2064, doi: 10.1093/mnras/stad1839

Cassanelli, T., Leung, C., Sanghavi, P., et al. 2024, Nature Astronomy, 8, 1429, doi: 10.1038/s41550-024-02357-x

Chatterjee, S., Law, C. J., Wharton, R. S., et al. 2017, Nature, 541, 58, doi: 10.1038/nature20797

Chen, X.-L., Tsai, C.-W., Li, D., et al. 2025, The Astrophysical Journal Letters, 980, L24, doi: 10.3847/2041-8213/adadfd

Connor, L., Ravi, V., Sharma, K., et al. 2025, Nature Astronomy, doi: 10.1038/s41550-025-02566-y

Cordes, J. M., & Chatterjee, S. 2019, ARA&A, 57, 417, doi: 10.1146/annurev-astro-091918-104501

Cordes, J. M., & Lazio, T. J. W. 2002, arXiv e-prints, astro, doi: 10.48550/arXiv.astro-ph/0207156

Cordes, J. M., & Lazio, T. J. W. 2003, NE2001. II. Using Radio Propagation Data to Construct a Model for the Galactic Distribution of Free Electrons. https://arxiv.org/abs/astro-ph/0301598

Cordes, J. M., Ocker, S. K., & Chatterjee, S. 2022, ApJ, 931, 88, doi: 10.3847/1538-4357/ac6873

Dav é , R., Angl é s-Alc á zar, D., Narayanan, D., et al. 2019, Monthly Notices of the Royal Astronomical Society, 486, 2827, doi: 10.1093/mnras/stz937

Deng, W., & Zhang, B. 2014, ApJL, 783, L35, doi: 10.1088/2041-8205/783/2/L35

Dolag, K., Gaensler, B. M., Beck, A. M., & Beck, M. C. 2015, Monthly Notices of the Royal Astronomical Society, 451, 4277, doi: 10.1093/mnras/stv1190

Driessen, L. N., Barr, E. D., Buckley, D. A. H., et al. 2024, MNRAS, 527, 3659, doi: 10.1093/mnras/stad3329

Foreman-Mackey, D., Hogg, D. W., Lang, D., & Goodman, J. 2013, PASP, 125, 306, doi: 10.1086/670067

FRB Collaboration, Amiri, M., Amouyal, D., et al. 2025, arXiv e-prints, arXiv:2502.11217, doi: 10.48550/arXiv.2502.11217

Fukugita, M., Hogan, C. J., & Peebles, P. J. E. 1998, ApJ, 503, 518, doi: 10.1086/306025

Gao, H., Li, Z., & Zhang, B. 2014, The Astrophysical Journal, 788, 189, doi: 10.1088/0004-637X/788/2/189

Glowacki, M., Lee-Waddell, K., Deller, A. T., et al. 2023, The Astrophysical Journal, 949, 25, doi: 10.3847/1538-4357/acc1e3

Gordon, A. C., Fong, W.-f., Kilpatrick, C. D., et al. 2023, ApJ, 954, 80, doi: 10.3847/1538-4357/ace5aa

Harris, C. R., Millman, K. J., van der Walt, S. J., et al. 2020, Nature, 585, 357, doi: 10.1038/s41586-020-2649-2

Hashimoto, T., Goto, T., On, A. Y. L., et al. 2020, MNRAS, 498, 3927, doi: 10.1093/mnras/staa2490

Heintz, K. E., Prochaska, J. X., Simha, S., et al. 2020, The Astrophysical Journal, 903, 152, doi: 10.3847/1538-4357/abb6fb

Hogg, D. W. 2000, Distance measures in cosmology. https://arxiv.org/abs/astro-ph/9905116

Hunter, J. D. 2007, Computing in Science & Engineering, 9, 90, doi: 10.1109/MCSE.2007.55

Ibik, A. L., Drout, M. R., Gaensler, B. M., et al. 2024, The Astrophysical Journal, 961, 99, doi: 10.3847/1538-4357/ad0893

Inoue, S. 2004, MNRAS, 348, 999, doi: 10.1111/j.1365-2966.2004.07359.x

Ioka, K. 2003, The Astrophysical Journal, 598, L79, doi: 10.1086/380598

James, C. W., Prochaska, J. X., Macquart, J.-P., et al. 2021, Monthly Notices of the Royal Astronomical Society, 509, 4775, doi: 10.1093/mnras/stab3051

Kalita, S., Bhatporia, S., & Weltman, A. 2024, arXiv e-prints, arXiv:2410.01974, doi: 10.48550/arXiv.2410.01974

Katz, J. I. 2018, Progress in Particle and Nuclear Physics, 103, 1, doi: 10.1016/j.ppnp.2018.07.001

Kaur, B., Kanekar, N., & Prochaska, J. X. 2022, The Astrophysical Journal Letters, 925, L20, doi: 10.3847/2041-8213/ac4ca8

Kumar, A., Maan, Y., & Bhusare, Y. 2024, ApJ, 977, 177, doi: 10.3847/1538-4357/ad84de

Law, C. J., Butler, B. J., Prochaska, J. X., et al. 2020, The Astrophysical Journal, 899, 161, doi: 10.3847/1538-4357/aba4ac

Lee-Waddell, K., James, C. W., Ryder, S. D., et al. 2023, PASA, 40, e029, doi: 10.1017/pasa.2023.27

Li, Y., Zhang, S. B., Yang, Y. P., et al. 2025, arXiv e-prints, arXiv:2503.04727, doi: 10.48550/arXiv.2503.04727

Li, Z., Gao, H., Wei, J. J., et al. 2020, MNRAS, 496, L28, doi: 10.1093/mnrasl/slaa070

Lin, H.-N., & Zou, R. 2023, Monthly Notices of the Royal Astronomical Society, 520, 6237, doi: 10.1093/mnras/stad509

Longair, M. S. 2023, Galaxy Formation (Springer), doi: 10.1007/978-3-662-65891-8

Lorimer, D. R., Bailes, M., McLaughlin, M. A., Narkevic, D. J., & Crawford, F. 2007, Science, 318, 777, doi: 10.1126/science.1147532

Macquart, J. P., Prochaska, J. X., McQuinn, M., et al. 2020, Nature, 581, 391, doi: 10.1038/s41586-020-2300-2

Mahony, E. K., Ekers, R. D., Macquart, J.-P., et al. 2018, The Astrophysical Journal Letters, 867, L10, doi: 10.3847/2041-8213/aae7cb

Marcote, B., Nimmo, K., Hessels, J. W. T., et al. 2020, Nature, 577, 190, doi: 10.1038/s41586-019-1866-z

McQuinn, M. 2013, The Astrophysical Journal Letters, 780, L33, doi: 10.1088/2041-8205/780/2/L33

Medlock, I., Nagai, D., Anglés-Alcázar, D., & Gebhardt, M. 2025, ApJ, 983, 46, doi: 10.3847/1538-4357/adbc9c

Michilli, D., Bhardwaj, M., Brar, C., et al. 2023, The Astrophysical Journal, 950, 134, doi: 10.3847/1538-4357/accf89

Nelson, D., Springel, V., Pillepich, A., et al. 2019, Computational Astrophysics and Cosmology, 6, 2, doi: 10.1186/s40668-019-0028-x

Ni, Y., DiMatteo, T., Bird, S., et al. 2022, Monthly Notices of the Royal Astronomical Society, 513, 670, doi: 10.1093/mnras/stac351

Niu, C. H., Aggarwal, K., Li, D., et al. 2022, Nature, 606, 873, doi: 10.1038/s41586-022-04755-5

Ocvirk, P., Aubert, D., Sorce, J. G., et al. 2020, Monthly Notices of the Royal Astronomical Society, 496, 4087, doi: 10.1093/mnras/staa1266

Petroff, E., Hessels, J. W. T., & Lorimer, D. R. 2019, The Astronomy and Astrophysics Review, 27, 4, doi: 10.1007/s00159-019-0116-6

Petroff, E., Hessels, J. W. T., & Lorimer, D. R. 2022, A&A Rv, 30, 2, doi: 10.1007/s00159-022-00139-w

Planck Collaboration, Aghanim, N., Akrami, Y., et al. 2020, A&A, 641, A6, doi: 10.1051/0004-6361/201833910

Platts, E., Weltman, A., Walters, A., et al. 2019, Physics Reports, 821, 1, doi: https://doi.org/10.1016/j.physrep.2019.06.003

Popov, S. B., Postnov, K. A., & Pshirkov, M. S. 2018, Physics-Uspekhi, 61, 965, doi: 10.3367/ufne.2018.03.038313

Press, W. H., & Schechter, P. 1974, ApJ, 187, 425, doi: 10.1086/152650

Price, D. C., Flynn, C., & Deller, A. 2021, PASA, 38, e038, doi: 10.1017/pasa.2021.33

Prochaska, J. X., & Zheng, Y. 2019, MNRAS, 485, 648, doi: 10.1093/mnras/stz261

Prochaska, J. X., Macquart, J.-P., McQuinn, M., et al. 2019, Science, 366, 231, doi: 10.1126/science.aay0073

Rajwade, K. M., Bezuidenhout, M. C., Caleb, M., et al. 2022, MNRAS, 514, 1961, doi: 10.1093/mnras/stac1450

Rajwade, K. M., Driessen, L. N., Barr, E. D., et al. 2024, MNRAS, 532, 3881, doi: 10.1093/mnras/stae1652

Ravi, V., Catha, M., D'Addario, L., et al. 2019, Nature, 572, 352, doi: 10.1038/s41586-019-1389-7

Ravi, V., Law, C. J., Li, D., et al. 2022, MNRAS, 513, 982, doi: 10.1093/mnras/stac465

Ravi, V., Catha, M., Chen, G., et al. 2023, ApJL, 949, L3, doi: 10.3847/2041-8213/acc4b6

Ravi, V., Catha, M., Chen, G., et al. 2025, The Astronomical Journal, 169, 330, doi: 10.3847/1538-3881/adc725

Rybicki, G. B., & Lightman, A. P. 1979, Radiative processes in astrophysics

Scott, D. R., Dial, T., Bera, A., et al. 2025, arXiv e-prints, arXiv:2505.17497, doi: 10.48550/arXiv.2505.17497

Shannon, R. M., Bannister, K. W., Bera, A., et al. 2025, PASA, 42, e036, doi: 10.1017/pasa.2025.8

Sharma, K., Krause, E., Ravi, V., et al. 2025, ApJ, 989, 81, doi: 10.3847/1538-4357/adeca4

Sharma, K., Ravi, V., Connor, L., et al. 2024, Nature, 635, 61, doi: 10.1038/s41586-024-08074-9

Sherman, M. B., Connor, L., Ravi, V., et al. 2023, The Astrophysical Journal Letters, 957, L8, doi: 10.3847/2041-8213/ad0380

Sherman, M. B., Connor, L., Ravi, V., et al. 2024, ApJ, 964, 131, doi: 10.3847/1538-4357/ad275e

Shull, J. M., Smith, B. D., & Danforth, C. W. 2012, ApJ, 759, 23, doi: 10.1088/0004-637X/759/1/23

Takahashi, R., Ioka, K., Mori, A., & Funahashi, K. 2021, MNRAS, 502, 2615, doi: 10.1093/mnras/stab170

Team, T. P. D. 2023, pandas-dev/pandas: Pandas, v2.0.1, Zenodo, doi: 10.5281/zenodo.7857418

Tendulkar, S. P., Bassa, C. G., Cordes, J. M., et al. 2017, The Astrophysical Journal Letters, 834, L7, doi: 10.3847/2041-8213/834/2/L7

Tendulkar, S. P., Gil de Paz, A., Kirichenko, A. Y., et al. 2021, The Astrophysical Journal Letters, 908, L12, doi: 10.3847/2041-8213/abdb38

Thornton, D., Stappers, B., Bailes, M., et al. 2013, Science, 341, 53, doi: 10.1126/science.1236789

Villaescusa-Navarro, F., Anglés-Alcázar, D., Genel, S., et al. 2021, The Astrophysical Journal, 915, 71, doi: 10.3847/1538-4357/abf7ba

Virtanen, P., Gommers, R., Oliphant, T. E., et al. 2020, Nature Methods, 17, 261, doi: 10.1038/s41592-019-0686-2

Wang, Y.-Y., Gao, S.-J., & Fan, Y.-Z. 2025, ApJ, 981, 9, doi: 10.3847/1538-4357/adade8

Wes McKinney. 2010, in Proceedings of the 9th Python in Science Conference, ed. Stéfan van der Walt & Jarrod Millman, 56 – 61, doi: 10.25080/Majora-92bf1922-00a

Xiao, D., Wang, F., & Dai, Z. 2021, Science China Physics, Mechanics & Astronomy, 64, 249501, doi: 10.1007/s11433-020-1661-7

Xiao, D., Wang, F., & Dai, Z. 2022, arXiv e-prints, arXiv:2203.14198. https://arxiv.org/abs/2203.14198

Xu, C., Feng, Y., & Xu, J. 2025, ApJ, 988, 177, doi: 10.3847/1538-4357/ade5b5

Xu, J., & Han, J. L. 2015, Research in Astronomy and Astrophysics, 15, 1629, doi: 10.1088/1674-4527/15/10/002

Xu, J., Feng, Y., Li, D., et al. 2023, Universe, 9, 330, doi: 10.3390/universe9070330

Yamasaki, S., & Totani, T. 2020, The Astrophysical Journal, 888, 105, doi: 10.3847/1538-4357/ab58c4

Yao, J. M., Manchester, R. N., & Wang, N. 2017, ApJ, 835, 29, doi: 10.3847/1538-4357/835/1/29

Zhang, B. 2020, Nature, 587, 45, doi: 10.1038/s41586-020-2828-1

Zhang, B. 2023, Rev. Mod. Phys., 95, 035005, doi: 10.1103/RevModPhys.95.035005

Zhang, B. 2024, Annual Review of Nuclear and Particle Science, 74, 89, doi: 10.1146/annurev-nucl-102020-124444

Zhang, Y., Liu, Y., Yu, H., & Wu, P. 2025a, arXiv e-prints, arXiv:2504.06845, doi: 10.48550/arXiv.2504.06845

Zhang, Z. J., Yan, K., Li, C. M., Zhang, G. Q., & Wang, F. Y. 2021, ApJ, 906, 49, doi: 10.3847/1538-4357/abceb9

Zhang, Z. J., Nagamine, K., Oku, Y., et al. 2025b, arXiv e-prints, arXiv:2503.12741, doi: 10.48550/arXiv.2503.12741

Zhou, B., Li, X., Wang, T., Fan, Y.-Z., & Wei, D.-M. 2014, Phys. Rev. D, 89, 107303, doi: 10.1103/PhysRevD.89.107303

Zhuge, J., & Kalomenopoulos, M. 2026, FRB_GW_cosmo: A Pipeline for FRB and Joint GWs-FRB Cosmological Analyses, 1.0, Zenodo, doi: 10.5281/zenodo.20282512

Ziegler, J. J., Shapiro, P. R., Dawoodbhoy, T., et al. 2024, arXiv e-prints, arXiv:2411.02699, doi: 10.48550/arXiv.2411.02699